



A numerical study on hurricane-induced storm surge and inundation in Charleston Harbor, South Carolina

Machuan Peng,¹ Lian Xie,¹ and Leonard J. Pietrafesa²

Received 11 October 2004; revised 21 March 2006; accepted 6 April 2006; published 15 August 2006.

[1] A storm surge and inundation model is configured in Charleston Harbor and its adjacent coastal region to study the harbor's response to hurricanes. The hydrodynamic component of the modeling system is based on the Princeton Ocean Model, and a scheme with multiple inundation speed options is imbedded in the model for the inundation calculation. Historic observations (Hurricane Hugo and its related storm surge and inundation) in the Charleston Harbor region indicate that among three possible inundation speeds in the model, taking $C_t (gd)^{1/2}$ (C_t is a terrain-related parameter) as the inundation speed is the best choice. Choosing a different inundation speed in the model has effects not only on inundation area but also on storm surge height. A nesting technique is necessary for the model system to capture the mesoscale feature of a hurricane and meanwhile to maintain a higher horizontal resolution in the harbor region, where details of the storm surge and inundation are required. Hurricane-induced storm surge and inundation are very sensitive to storm tracks. Twelve hurricanes with different tracks are simulated to investigate how Charleston Harbor might respond to tracks that are parallel or perpendicular to the coastline or landfall at Charleston at different angles. Experiments show that large differences of storm surge and inundation may have occurred if Hurricane Hugo had approached Charleston Harbor with a slightly different angle. A hurricane's central pressure, radius of maximum wind, and translation speed have their own complicated effects on surge and inundation when the hurricane approaches the coast on different tracks. Systematic experiments are performed in order to illustrate how each of such factors, or a combination of them, may affect the storm surge height and inundation area in the Charleston Harbor region. Finally, suggestions are given on how this numerical model system may be used for hurricane-induced storm surge and inundation forecasting.

Citation: Peng, M., L. Xie, and L. J. Pietrafesa (2006), A numerical study on hurricane-induced storm surge and inundation in Charleston Harbor, South Carolina, *J. Geophys. Res.*, *111*, C08017, doi:10.1029/2004JC002755.

1. Introduction

[2] The Charleston region is known for its port, one of the largest along the South Carolina coast. (Figure 1a). The highly populated Charleston Peninsula (where the city of Charleston is located) is formed by the juncture of the Cooper, Ashley, and Wando Rivers, which meet in Charleston Harbor.

[3] The outer shore of the harbor is composed of recently, geologically developed barrier islands, including Isle of Palms, Sullivans Island, Scanlonville, James Island, Morris Island, Folly Beach, and Kiawah Island, all of which are characterized by elevations of less than 3 m and averaging about 2 m above mean sea level (MSL). Sheltered by the barrier islands are extensive intertidal salt marsh/tidal creek

systems. The area west of the Ashley River near the Charleston Peninsula is very flat, with elevations generally below 3 m. The highest inland area within the study region is located on both sides of the Cooper River, and to the north and northwest of the Wando River system, and ranges from 6 to 9 m (Figure 1b). The bathymetry in most of the Charleston Harbor area is around 5 m. Only at its entrance does the water depth reach up to 10 m. On the shelf, water depth increases gradually away from the coast.

[4] The total surface area of the Charleston Harbor system is approximately 112 km², with a mean depth of 3.7 m at mean low water (MLW), a maximum depth of 10 m, with the water volume estimated to be 0.84 km³ at mean tidal elevation [Kjerfve *et al.*, 1978]. The harbor mouth is about 2500 m in width. The Cooper River dominates the discharge into the harbor, with an average flow of 122 m³/s. The mean combined discharge of the Ashley and Wando Rivers is less than 10 m³/s.

[5] The tidal range increases slightly from north to south along the outer shoreline. Charleston's mean tidal range is 1.6 m; spring tides average 1.9 m; and the highest astro-

¹Department of Marine, Earth, and Atmospheric Sciences, North Carolina State University, Raleigh, North Carolina, USA.

²College of Physical and Mathematical Sciences, North Carolina State University, Raleigh, North Carolina, USA.

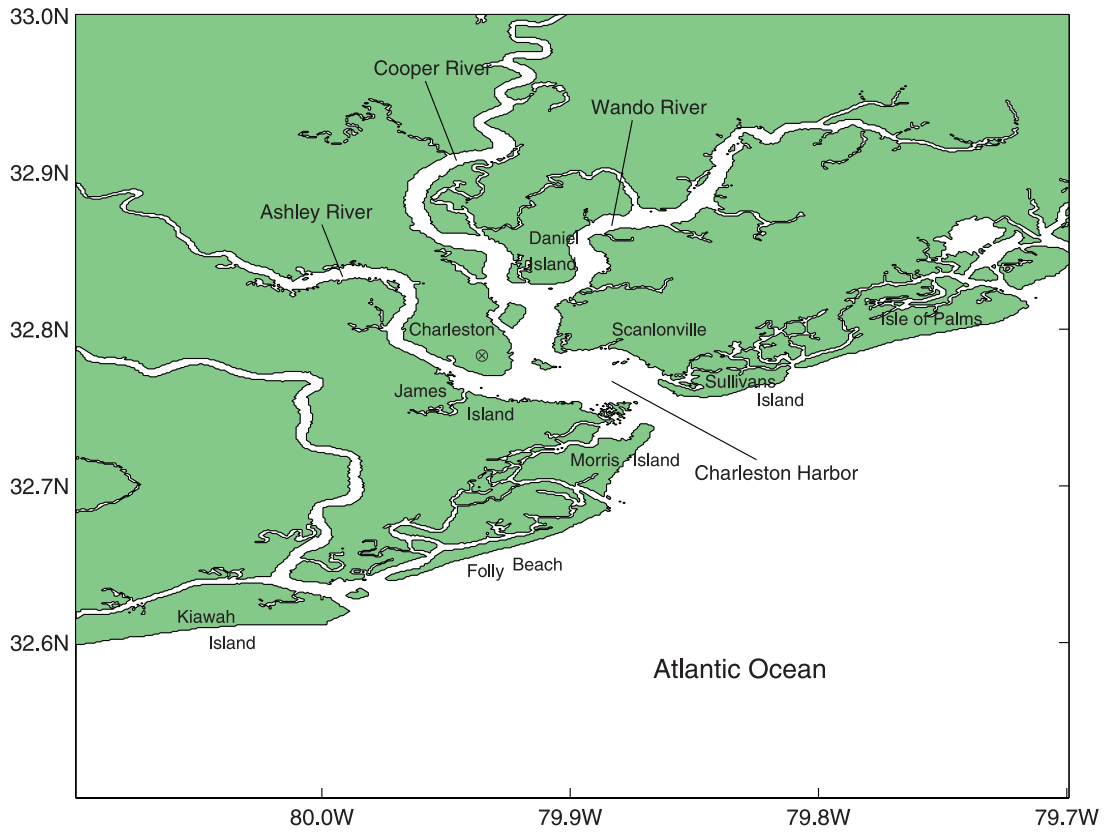


Figure 1a. Charleston Harbor and its adjacent coastal area, showing names and locations.

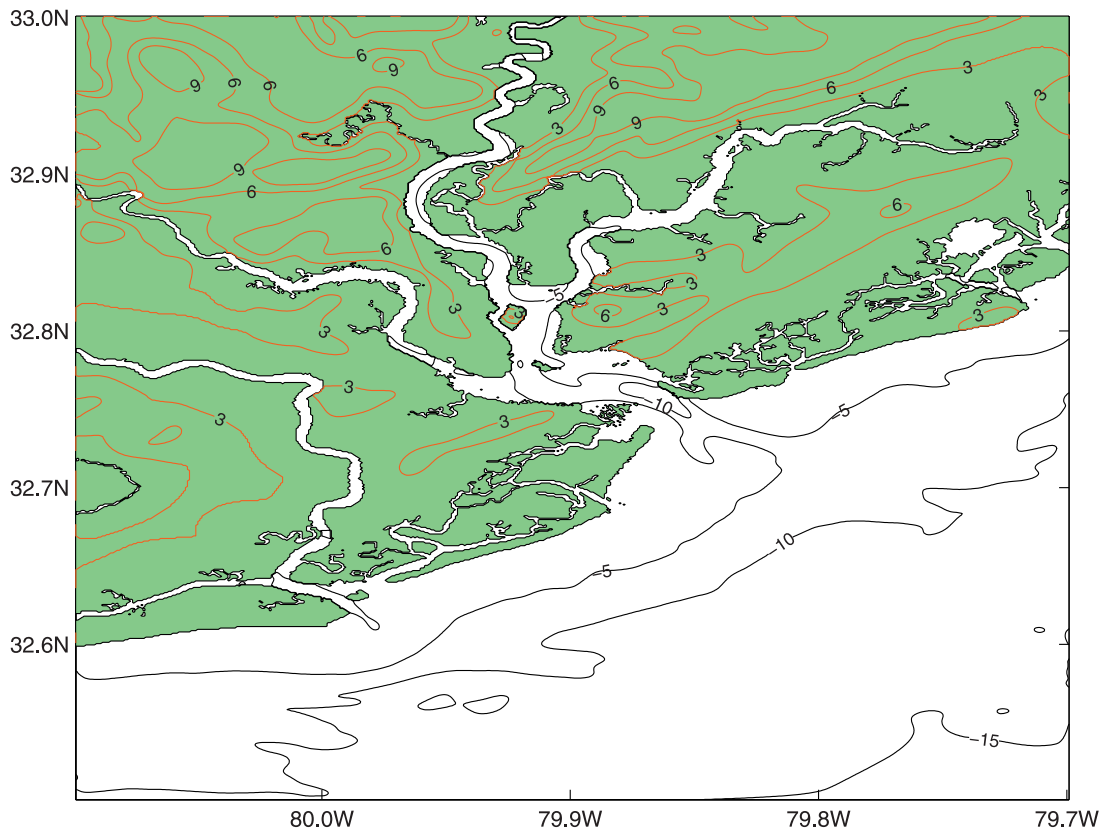


Figure 1b. Charleston Harbor and its adjacent coastal area, showing bathymetry and land elevation (in meters with mean sea level (MSL) as the vertical datum).

nomie tide of the year is about 2.1 m. The wave climate at Charleston is dependent on offshore swell conditions but is diurnally modified by the sea breeze/land breeze cycle typical to the region. Breaking wave height along the outer beaches is approximately 60 cm in the Charleston area [Finley, 1976].

[6] The Charleston region experiences several types of high-energy, short-term natural hazards. The two most prominent are earthquakes and tropical cyclones (TCs). While earthquakes are very infrequent, hurricanes and tropical storms affect the study domain annually. Many of these TCs have been severe hurricanes and some have individually claimed hundreds of lives and leveled buildings across the Charleston Harbor area. For example, 4 m storm surges were recorded during the 1893 and 1911 hurricanes, and a 5 m surge was measured during a 1852 hurricane (Naval Meteorology and Oceanography Operational Support, Tropical cyclones affecting Charleston, 2003, available at <https://www.cnmoc.navy.mil/nmosw/tr8203nc/charlsto/text/frame.htm>). Hurricane Hugo (22 September 1989) produced a record high storm tide of 6 m along the offshore part of the coast to the northeast of the entrance to Charleston Harbor. Inside the harbor, a record high surge of 3.3 m was also measured at the Charleston Tide Gauge Station [National Oceanic and Atmospheric Administration (NOAA), 1989]. While this Safir/Simpson Category Four hurricane incurred in excess of \$7 billion in damage [NOAA, 1989], the well-documented hurricane track, central pressure, and radius of maximum wind (RMW) measurements have great value in ground-truthing and validating the numerical storm surge and inundation models.

[7] Numerical studies of hurricane-induced storm surge began in the early 1970s. The best known model for predicting open-coast hurricane-surge elevations was the National Oceanic and Atmospheric Administration's (NOAA's) Special Program to List Amplitudes of Surges from Hurricanes or "SPLASH" [Jelesnianski, 1972]. Later, Sea, Lake, and Overland Surges from Hurricanes or "SLOSH," was developed [Jelesnianski et al., 1984; Jelesnianski et al., 1992] and has been widely used by NOAA for coastal flooding and inundation forecasts along the Gulf Coast and Eastern Seaboard of the United States, including the Charleston Harbor region.

[8] The two-dimensional SLOSH was designed for forecasting hurricane-induced storm surge and inundation along a large portion of the coast, in effect creating a "coarsely" depicted scenario of what will happen. The model was built to capture the major features of the coastal response to the Safir-Simpson categories of hurricanes, and thus is not ideal for the study of a specific hurricane event in a particular forecast domain. SLOSH does not incorporate the advection terms explicitly in the model's momentum equations [Jelesnianski et al., 1992]. This is not a big problem for the open ocean and the outer continental shelf where water depths are relatively large and horizontal spatial gradients of currents are small. However, for the inner-shelf coastal region where water depths are shallow and the contour of the sea-land boundary is complicated, strong nonlinear effects should not be neglected in the model.

[9] Hubbert and McInnes [1999] (hereinafter referred to as the HM scheme) retained the advection terms in the momentum equations in their model, so nonlinear effects

were no longer assumed small in comparison with the Coriolis effect as is assumed in SLOSH. As a result, strong nonlinear effects in shallow regions, or in places where the bathymetry gradient is great, are more accurately reflected in their model. This merit was demonstrated when storm-induced surge and inundation were simulated for a tropical cyclone and two separate cold fronts that passed along the Australian coast [Hubbert and McInnes, 1999]. However, the HM scheme is also two-dimensional, thus prone to underestimate the height of storm surge [Pietrafesa et al., 1986] and the subsequent inundation. Furthermore, using the vertically averaged velocity as the inundation speed, as suggested in the HM scheme, is more likely to underestimate the interface moving speed of the sea-land boundary [Peng et al., 2004], and so to underestimate the inundation area.

[10] Xie et al. [2004] (hereinafter referred to as the XPP model) introduced a modified version of the HM scheme that incorporates mass conservation and the flexibility to choose inundation speed on the basis of three-dimensional flow fields. This new scheme was incorporated into a three-dimensional storm surge model. Experiments under idealized geometry and forcing conditions revealed the need to impose mass conservation and to properly set the inundation speed for modeling in closed or semiclosed coastal systems, such as lakes and sounds. This model was applied to the Croatan-Albemarle-Pamlico Estuary System (CAPES), and the storm surge and inundation area were simulated when fictitious Category Two and Category Three hurricanes passed along hypothetical paths in the CAPES [Peng et al., 2004]. The response of the CAPES to actual historic hurricanes was also simulated in their study, and the simulated storm surge along the coast agreed well with observations. However, there were only a few locations where measured data were available.

[11] It is fair to say that, in general, inundation records that can be used to validate inundation part of the model are even much scantier. Better ground-truth is needed and further validation of the numerical model in general, and of inundation speed and scope in particular is required. In addition, the CAPES is a nearly closed lagoon system with limited interaction with the open ocean. To show if the XPP model is robust for all types of coastal regions, a more open estuary or bay like Charleston Harbor needs to be tested.

[12] In this paper, the XPP model will be deployed in the Charleston Harbor and its adjacent shelf. To accurately represent the complicated topographic features of the harbor, especially in the vicinity of downtown Charleston where three rivers converge, a high horizontal resolution database has to be used. Further, since the Radius of Maximum Wind has been found to be about 50 km for the robust Atlantic Coast hurricanes [Hsu and Yan, 1998], and the total surface area of the Charleston Harbor is only 112 km², a calculation domain larger than the harbor is needed to obtain reliable model output. Choosing a smaller domain would underestimate the surge height and thus underestimate the inundation area in the harbor. Given the above, a spatial nesting technique is introduced.

[13] Generally, models can be nested in order to increase horizontal resolution in a focused subregion of the model domain, without incurring the computational expense of high resolution over the entire model domain. Nested

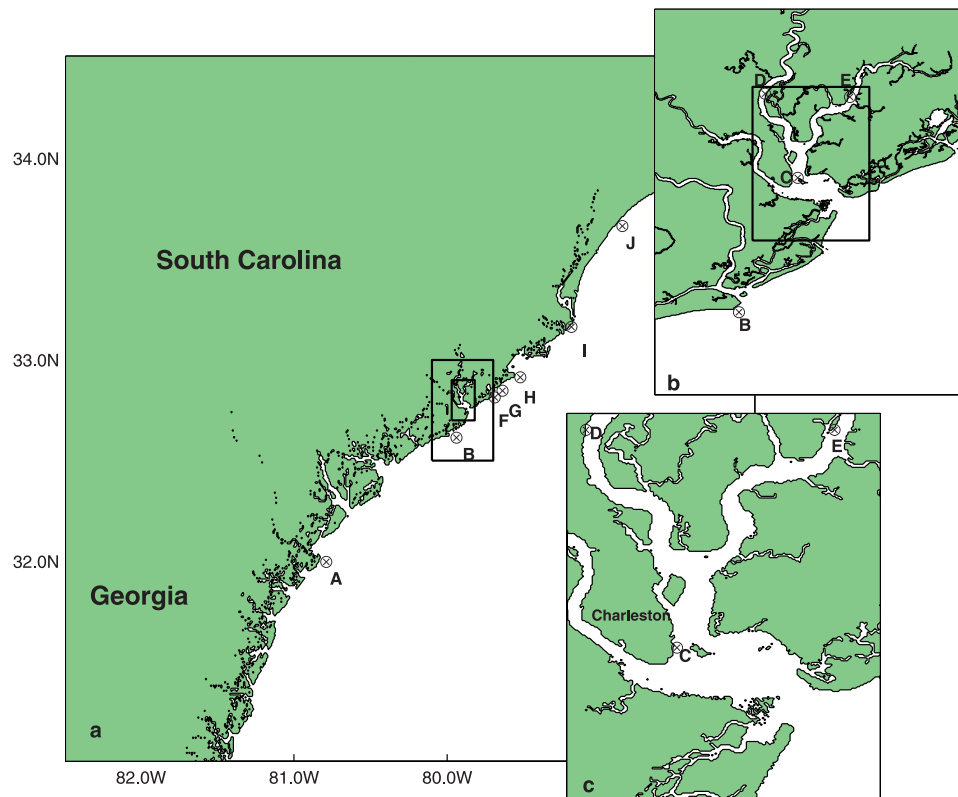


Figure 2. (a–c) The 3 nesting domains and the 10 coast storm surge stations, for the outer, middle, and inner domains in the model, respectively. A, B, C, D, E, F, G, H, I, and J are the sea level stations. The observation feature of each individual station can be found in Table 1.

models fall into two categories, passive and interactive [Spall and Holland, 1991], or simply called one-way and two-way [Fox and Maskell, 1995]. Passive, or one-way, nested models use boundary conditions for the high-resolution region that have been obtained from a previous low-resolution calculation. Interactive, or two-way, models in addition to providing boundary conditions for the fine grid region, allow the evolution within the fine grid to influence the evolution on the coarse grid [Spall and Holland, 1991]. As the spatial scales of hurricanes are far larger than that of Charleston Harbor, and the passage energy propagation generally follows the direction of the storm, (i.e., from outer domain to inner domain) the one-way nesting is deemed adequate and used in this study for the simulation of the harbor's hydrodynamic response to hurricane forcing, including the hindcasted response to Hurricane Hugo.

[14] The manuscript is organized as follows. In section 2 the storm surge and inundation modeling system and its configuration for Charleston Harbor are briefly described. Section 3 describes the Hurricane Hugo wind model and the subsequent simulated storm surge and inundation results with the invoked XPP inundation model. Section 4 discusses different inundation schemes and illustrates the need to further improve the existing inundation architecture. The size effect of the outer domain is assessed in section 5. Storm surge and inundation produced by various hypothetical hurricanes are calculated in section 6 to demonstrate the hydrodynamic responses of Charleston Harbor to varying

hurricane tracks. Finally, conclusions and discussion are given in section 7.

2. Model Configuration in the Charleston Harbor Domain

[15] The storm surge and inundation modeling system used in this study is described in detail by Xie *et al.* [2004] and Peng *et al.* [2004]. The hydrodynamic component of the modeling system is based on the Princeton Ocean Model (POM) [Mellor, 1996], which uses a terrain-following sigma (σ) coordinate in the vertical and a staggered Arakawa C grid in the horizontal plane. An embedded second moment turbulence closure submodel is used to compute the vertical mixing coefficients. The model uses a free surface, and thus allows an explicit prediction of sea level change. In POM, the horizontal finite differencing is explicit, whereas the vertical differencing is implicit. The latter eliminates time step constraints on the vertical resolution and permits the use of fine vertical resolution near the surface and in shallow water regions. A three-time level leapfrog scheme is used for temporal integration.

[16] Atmospheric forcing for the model is computed externally. It is imposed on the system via surface boundary conditions, which include wind stress and pressure perturbations. Additional surface boundary conditions in the form of heat, moisture, radiation, precipitation, and evaporation fluxes can also be imposed, but are not used for the storm surge modeling presented within. Lateral boundary condi-

tions include an open boundary in the coastal ocean that permits surface waves to propagate out of the model domain to prevent energy accumulation along the boundary. On the land side of the model domain, runoffs from major rivers can be prescribed, but are not used in this study.

[17] In the XPP model, to determine whether or not a land grid point will be inundated, the sea surface elevation at any wet grid cell adjacent to it is compared to the elevation of the land grid point. If the water is higher than the land elevation, then flooding is possible and a second criterion is examined. The distance water could travel across the “flooding-in-action” grid cell in a single time step is computed using the inundation speed at the location. The distance is integrated over time. If it is larger than the grid size, then the grid cell turns into water, that is, it is flooded. Otherwise, flooding does not occur. One of the modifications made to the HM scheme is in the choice of the inundation speed. In the HM scheme the inundation speed is determined by the value of vertically averaged currents, whereas in the XPP model, the inundation speed is the surface current derived from the three-dimensional model. This modified scheme is shown to work well in the CAPES, a semi-enclosed lagoon system [Peng *et al.*, 2004]. Its applicability in a relatively open body of water like Charleston Harbor will be assessed in this study.

[18] The storm surge and inundation modeling system is configured in Charleston Harbor and its adjacent shelf. In order to resolve the hydrodynamics of the relatively small harbor, a nesting system of three domains (Figure 2) is deployed. The outer domain is 78.0–82.5°W, 31.0–34.5°N with 1 minute (or $\Delta y = 1853$ m, and $\Delta x = \Delta y \cdot \cos \theta$, where θ is the latitude at the cell center) as the spatial grid size for both directions. The reason for choosing such a large region as the outer domain will be illustrated in section 5. The middle domain is 79.7–80.1°W, 32.5–33.0°N, with 12 s as the spatial grid size (1/5 of the outer grid size). The inner domain, providing detailed information in and around Charleston Harbor, covers 79.75–80.00°W, 32.70–32.90°N, with 3 s as the spatial grid size (1/20 of the outer grid size). In the vertical, four sigma levels are used for all domains. The bathymetry and land elevation are obtained and interpolated from the GEODAS publication (version 4.0.7 at <http://www.ngdc.noaa.gov/mgg/gdas>). MLW (mean low water) is the original vertical datum for both land elevation and bathymetry. Readjustment will be performed when MSL or NGVD (National Geodetic Vertical Datum) is required as the vertical datum.

[19] Time step, based on the grid size of the model (with constrain of CFL criterion), is important for the inundation scheme. In our nesting system, time steps for the outer, middle, and inner domains are respectively 120, 30, and 5 s. The time step for each domain is small enough to ensure that the corresponding grid cell may not be inundated at one time. In other words, the selection of time steps will not “artificially” slow down the inundation speed in all nesting domains.

3. Hurricane Hugo (1989)

[20] Hurricane Hugo affected Charleston Harbor, South Carolina, on 21–22 September 1989 as a Category 4 hurricane. The landfall location was merely 20 km to the

northeast of Downtown Charleston. The storm surge effects were severe; the maximum elevations recorded at water level stations close to the hurricane track exceeded the recorded highest water elevations [NOAA, 1989]. This historic hurricane left well-documented records of storm surge and inundation. These valuable data, along with recorded hourly central pressure and other meteorological measurements, provided important information for model validation.

3.1. Hurricane Track and Structure

[21] The eye of Hurricane Hugo entered the outer model domain at 09/21/2130Z and exited at about 22/0830Z. The landfall time was near 22/0400Z, with central pressure of 946 mbar. The lowest recorded pressure for the event was 934 mbar, which occurred just a few hours before landfall. The details of its track and the associated central pressure are illustrated in Figure 3. Interpolation was performed to calculate the central pressure at each time step.

[22] The hurricane pressure and surface wind fields were calculated following Holland [1980]:

$$P = P_c + (P_n - P_c) \exp(-A/r^B) \quad (1)$$

$$V'_w = [AB(P_n - P_c) \exp(-A/r^B) / (\rho r^B)]^{1/2} \quad (2)$$

where ρ is the air density, P is the atmospheric pressure at radius r , P_c is the hurricane central pressure, P_n is the ambient pressure, A and B are scaling parameters, and V'_w is the hurricane pressure gradient induced wind velocity. Those parameters are set to: $P_n = 1010$ mbar, $\rho = 1.2$ kg/m³, $B = 1.9$, $A = (R_{\max})^B$, where R_{\max} is the radius of maximum wind (RMW), which is linearly interpolated from the measured values. The wind speed used in this study is the combination of equation (2) and hurricane translation speed V_H :

$$\vec{V}_w = \vec{V}'_w + \vec{V}_H \quad (3)$$

Hurricane wind stress is computed using the conventional bulk formula:

$$\tau = \rho C_d |\vec{V}_w| \vec{V}_w \quad (4)$$

where C_d is the drag coefficient, which is assumed to vary with wind speed [Large and Pond, 1981]:

$$10^3 C_d = \begin{cases} 0.49 + 0.065 |\vec{V}_w| & |\vec{V}_w| \geq 10 \text{ m/s} \\ 1.14 & 3 \leq |\vec{V}_w| < 10 \text{ m/s} \\ 0.62 + 1.56/|\vec{V}_w| & 1 \leq |\vec{V}_w| < 3 \text{ m/s} \\ 2.18 & |\vec{V}_w| < 1 \text{ m/s} \end{cases} \quad (5)$$

[23] The parametric wind model, assuming a circular wind flow pattern around its center, does not adequately reflect the actual surface wind directions, and wind inflow

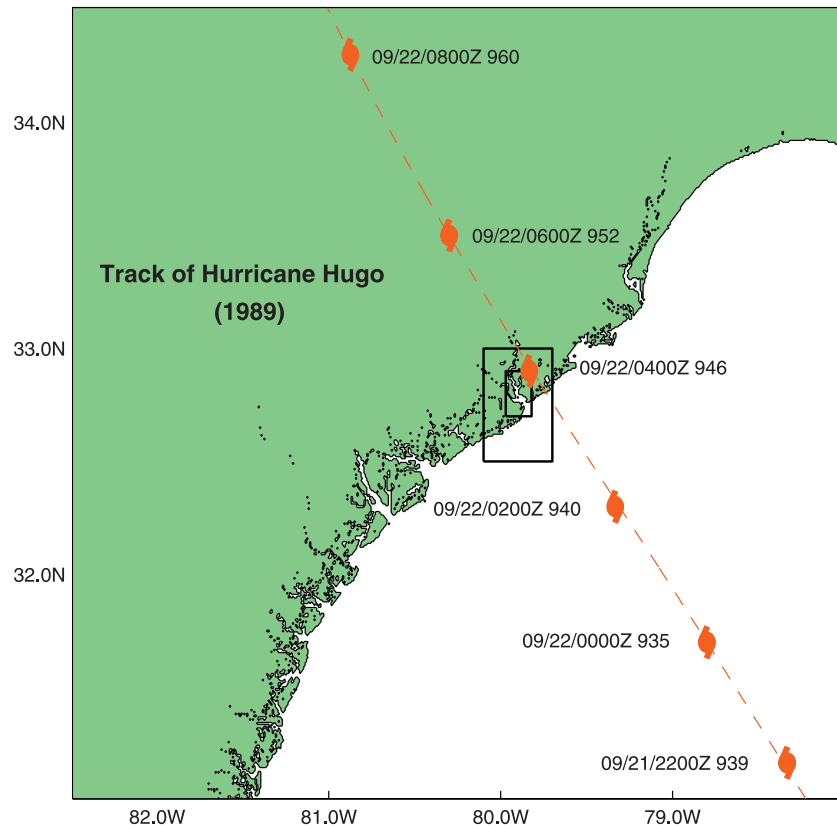


Figure 3. The track of Hurricane Hugo in the outer domain with eye location and central pressure (in mbar) shown every 2 hours from 09/21/2200Z to 09/22/0800Z.

angles must be considered in the model. In this study, the inflow angle varies linearly from 10° at the hurricane center to 20° at R_{\max} , and then increases linearly to 25° at $1.2 R_{\max}$, and remains at 25° beyond $1.2 R_{\max}$ [Phadke *et al.*, 2003]. This inflow angle structure pattern remains the same for Hurricane Hugo and all the assumed hurricanes in the paper. Of course, the inflow angle pattern of a real hurricane may be, to some extent, different from the assumed structure in the model [Houston *et al.*, 1999].

[24] No digital wind data are available to compare the model generated wind field with the observation at each time. However, the general pattern of the overall maximum wind speed by model agrees quite well with the historic document. For instance, the model indicates that before landfall the maximum wind occurred in the hurricane's northeastern quadrant. Along the coast, a maximum of 55 m/s wind speed existed between Sullivan's Island and Isle of Palms, or about 40 km to the northeast of the landfall location. In the southwestern quadrant, a 50 m/s high-speed region was found at Morris Island. This maximum wind speed distribution agrees well with the documented wind of Hurricane Hugo at <http://www.nhc.noaa.gov/gifs/1989hugo.gif>.

3.2. Storm Surge and Inundation

[25] The inundation scheme developed by Xie *et al.* [2004] was applied to the nesting system. The model output was compared with observations to investigate if the model works well for an estuary area with a relatively large open

entrance. Astronomical tide during the hurricane event was simulated on the basis of the harmonic constants of the six major partial tides in the study region (M2, N2, K2, M1, O1, and K1). Along the open boundary, sea level oscillation, $\zeta(t) = \sum A_i \cos(\omega_i t - \theta_i)$, was employed as the only exterior driving force in the model, where A_i , ω_i and θ_i are respectively the amplitude, speed, and Greenwich epoch of the individual partial tide. The simulated astronomical tides in every 6 minute were stored for the purpose of obtaining storm tide.

[26] The results show that the simulated storm tide (storm surge + astronomical tide) agrees well with observations. The periodical astronomical tide at each station was added to the simulated storm surge to make storm tide. As indicated in Figure 4, moving from south to north along the coast, the maximum storm tide increases from station A to H, where the peak is reached, and then decreases thereafter, with the only exceptions at stations D and E where the values are smaller than their neighbors. This is because these two stations are at the lower reaches of the Cooper and Wando Rivers. The distribution of the maximum storm surge along the coast is almost the same as the trend shown in Figure 4 owing to the fact that the amplitude (half range) difference of the M2 tide (the major partial tide of the region) from A to J is less than 0.5 m (Center for Operational Oceanographic Products and Services (CO-OPS), <http://www.co-ops.nos.noaa.gov/>). The locations and features of the stations can be found in Table 1, which indicates that 4 out of 10 are high water mark (HWM)

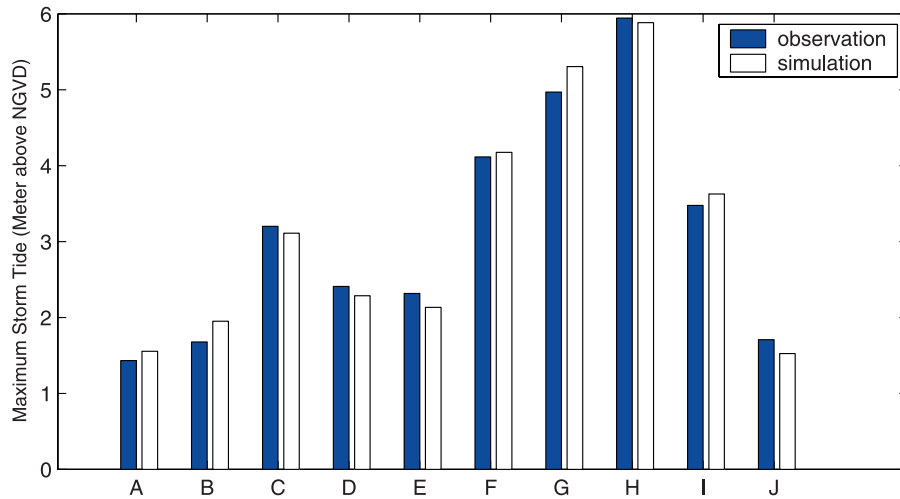


Figure 4. The observed and simulated maximum storm tide above National Geodetic Vertical Datum (NGVD) of Hurricane Hugo at 10 coastal stations.

stations [NOAA, 1989]. The reliability of the HWM data is not as good as the tidal gauge stations. For instance, in Table 2, which is a small clip of a long list of all HWM data records of Hurricane Hugo (the total HWM number is around 350), Awendaw7 and Awendaw8 are less than 1 km away, but the HWM difference is more than 1 m. Such records are apparently not reliable, though their data quality is claimed to be in “good” status. The similar low reliability of the HWM data appears at stations of Sewee Bay13 and Sewee Bay14. Discretion had been taken to avoid inclusion of such low reliable cases when the HWM stations were selected for Table 1.

[27] To further investigate the reliability and accuracy of the model for storm surge simulation, the calculated storm surges from 09/21/06:00Z to 09/23/04:00Z were chosen at stations A, C, and I to compare with the measured time series. The comparison is shown in Figure 5, which indicates that the model output agrees well with observations not only for peak values but also for phases. In Figure 5 the periodical astronomical tide at the three stations was removed from the original measured sea level data to make the observed curves. When Hurricane Hugo made landfall around 4:00Z (or midnight for local daylight saving time) on 22 September at Sullivans Island (see Figures 1a and 1b for location), the

storm surge values at stations C and I were near their peaks, while the surge at A, a station about 100 km southwest to the landfall location, was close to the water level minimum, with a sea surface height of about 0.8 m lower than a normal condition (with astronomical tide only). This is because the anticlockwise rotating wind mechanically induced opposite sea surface responses along the coast on both sides of the hurricane center, or eye, as the hurricane approached land. The 2-m-plus storm surge at station C, riding on the astronomical high tide, indicated that the sea surface at the Charleston tidal gauge had surpassed the historic record high (the station has hourly sea level record from 1921). In fact, as shown in Figure 4, the storm surge height was much higher at stations F, G, and H. As there were no tidal gauges at those locations, no measured time series of sea level were available to compare with the calculated results.

[28] The simulated inundation area (Figure 6a) matches well with observations (Figure 6b) in most regions in Charleston Harbor and its adjacent coastal areas, as long as the location is not in the vicinity of the river systems. For example, the inundation area at Kiawah Island, Folly Beach, Morris Island, James Island, East Coast of Downtown Charleston, southern Daniel Island, most of Sullivans Is-

Table 1. Location and Features for Storm Surge Stations^a

Station Number	Station Name	Latitude	Longitude	Station Type
A (8670870)	Ft. Pulaski, GA	32°02.0'N	80°54.1'W	tide gauge
B	Legareville	32°38.7'N	80°03.9'W	HWM
C (8665530)	Charleston, SC	32°46.9'N	79°55.5'W	tide gauge
D (8664662)	Army Depot, SC	32°54.6'N	79°57.1'W	tide gauge
E (8664545)	Wando River, SC	32°55.6'N	79°49.8'W	tide gauge
F	Fort Moultrie	32°47.5'N	79°46.4'W	HWM
G	Fort Moultrie	32°50.2'N	79°46.9'W	HWM
H	Sewee Bay	32°57.5'N	79°39.5'W	HWM
I (8662746)	Winyah Bay, SC	33°14.1'N	79°12.2'W	tide gauge
J (8661139)	Bucksport, SC	33°38.8'N	79°05.7'W	tide gauge

^aA, C, D, E, I, and J are tide gauge stations with seven-digit identification numbers given by the National Oceanic and Atmospheric Administration (NOAA). B, F, G, and H are high water mark (HWM) stations measured after Hurricane Hugo. For all of these HWM data the quality is “good” or above [from NOAA, 1989].

Table 2. Some of the High Water Marks Collected After Hurricane Hugo, Where the Location and Quality of the Data are Listed^a

Name	Serial Number	Latitude	Longitude	HWM, m	Quality
Awendaw	7	33°01'19"	79°36'03"	5.12	good
Awendaw	8	33°00'56"	79°35'34"	6.16	good
Bull Island	1	32°54'29"	79°36'46"	4.94	good
Bull Island	2	32°54'27"	79°36'45"	4.94	good
Bull Island	3	32°54'27"	79°36'43"	4.94	good
Sewee Bay	1	32°58'08"	79°38'15"	5.94	fair
Sewee Bay	2	32°58'13"	79°38'15"	5.91	good
Sewee Bay	3	32°57'42"	79°39'02"	5.73	fair
Sewee Bay	4	32°57'29"	79°38'51"	5.73	good
Sewee Bay	5	32°57'28"	79°38'44"	6.00	good
Sewee Bay	6	32°57'20"	79°38'42"	5.91	good
Sewee Bay	7	32°57'20"	79°38'46"	6.10	good
Sewee Bay	8	32°57'16"	79°38'48"	6.16	good
Sewee Bay	9	32°56'29"	79°39'30"	5.88	good
Sewee Bay	10	32°56'29"	79°39'30"	5.73	good
Sewee Bay	11	32°55'56"	79°41'10"	4.94	fair
Sewee Bay	12	32°55'55"	79°41'09"	5.00	fair
Sewee Bay	13	32°55'10"	79°41'10"	5.55	good
Sewee Bay	14	32°52'36"	79°44'55"	4.63	good

^aThe high water marks are from NOAA [1989]. The vertical datum is National Geodetic Vertical Datum (NGVD).

land, and Isle of Palms agrees very well with observations (see Figures 1a and 1b for their locations). The model output of inundation area is underestimated in the upper reaches of the Ashley, Cooper, and Wando Rivers. This is

because hurricane-induced precipitation and the consequent river discharge increase are not considered in the model. [29] It should be noted that some of the underestimation of inundation is likely due to the limitation of the inundation

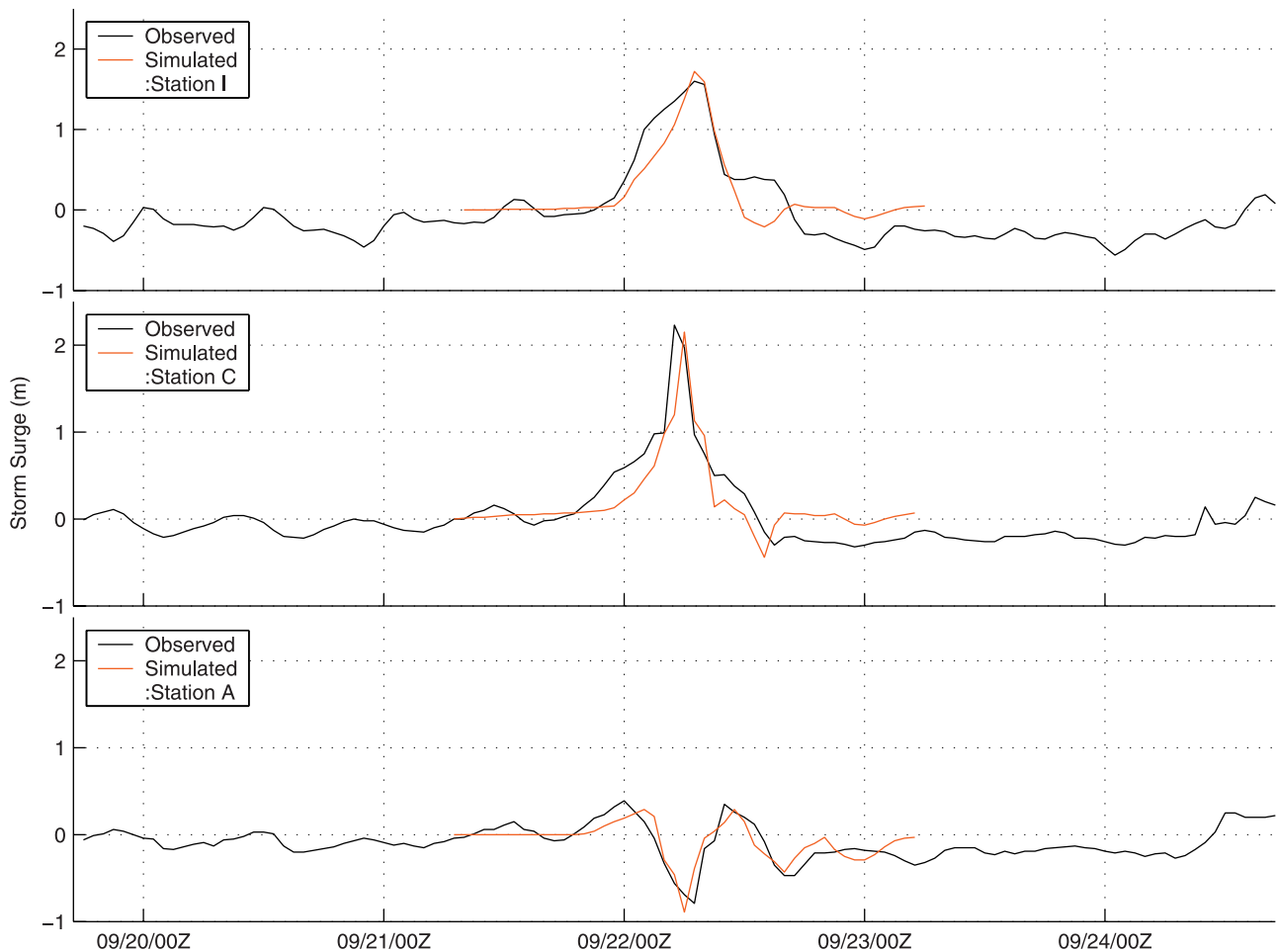


Figure 5. Observed and simulated time series of storm surge at stations A, C, and I induced by Hurricane Hugo.

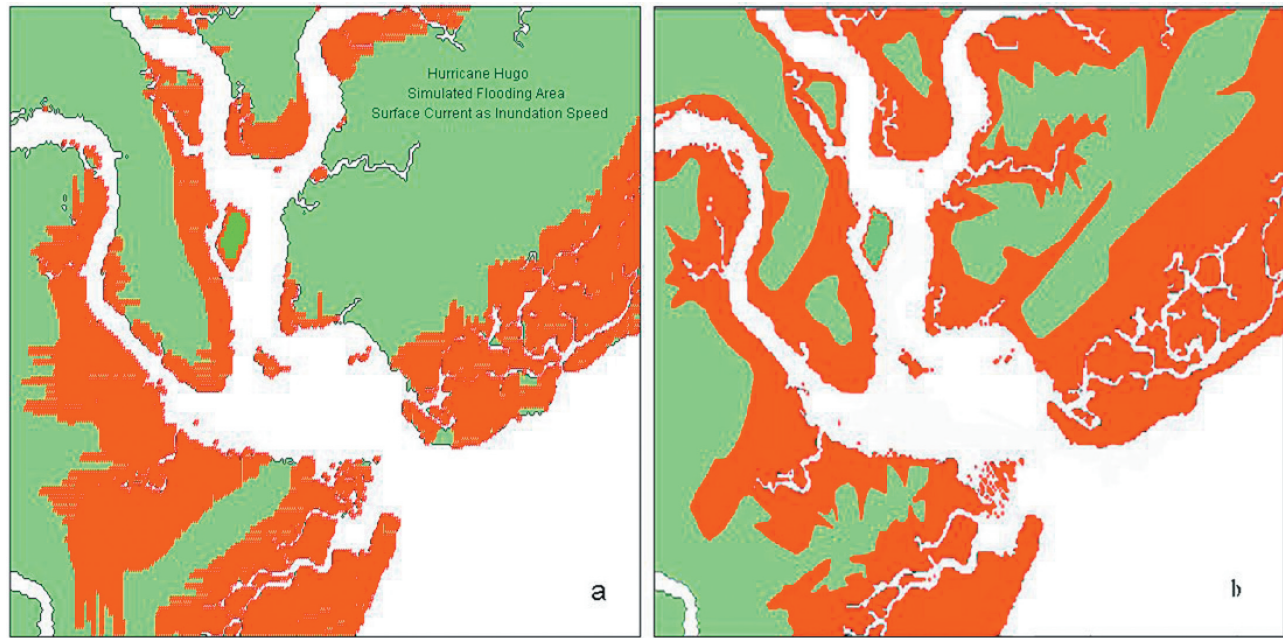


Figure 6. Comparison of the (a) model-simulated inundations of Hurricane Hugo and (b) observed inundations of Hurricane Hugo. The inundation area is shaded. Model results used surface current speed as the inundation speed.

scheme as will be discussed in section 4. The simulated maximum sea level on the west coast of Charleston, as will be shown later on, for instance, is at least 0.5 m higher than the land elevation at the same location (the land elevation along the coast of Charleston is less than 3 m in most area). Larger stretches of the coastal lands in the western part of Charleston are expected to be inundated than the simulated results shown in Figure 6a. The same evident inundation underestimation happens in the west part of Scanlonville and several locations of Sullivans Island, where the simulated maximum sea surface is also far above land elevation, but inundation does not occur as expected.

4. Inundation Schemes

4.1. Limitation of the Existing Inundation Scheme

[30] Though the *Xie et al.* [2004] model works well in a near-closed domain [Peng *et al.*, 2004], it does not accurately reflect the inundation area in some coastal areas in Charleston Harbor during Hurricane Hugo event. This is because, in such an open estuary, storm surge is generally influenced by the propagation into the harbor domain of long gravity waves produced by the hurricane in the open ocean. This is in contrast to what happens in closed or near-closed waters, in which response to wind-forcing tends to be local. In closed or near-closed waters, only the coast that is likely to gain water owing to local wind forcing may be inundated, where the direction of surface wind driven current is toward land. The XPP model, whose inundation speed control is based on surface current, can give a good inundation simulation in such cases.

[31] When the long gravity wave originating in the open ocean propagates to an open estuary like Charleston Harbor and the sea level surpasses the corresponding land elevation, inundation may take place not only on the coast that is

likely to gain water owing to local wind, but also on the coast that is subject to water loss (of course, such local wind induced water loss is less intense than the sea level increase owing to a long gravity wave propagating from the open ocean). In other words, sea surface elevation along the coast may far surpass the corresponding land elevation, with the surface current moving away from the land. The XPP model may underestimate the extent of coastal inundation in such a case.

[32] As mentioned before, in the XPP model, two requirements must be met before a land grid cell is inundated. The first requirement is that the sea surface elevation at a water grid cell must be higher than the land elevation of its neighboring land grid cell. The second is that the sea-land interface must complete the journey of a grid cell distance at a model recommended inundation speed. In their model, the surface current speed immediately adjacent to land is taken as the inundation speed. In Charleston Harbor the second requirement may not be met along the coast where the surface wind driven current is moving away from the land, even though the sea surface height far surpasses the corresponding land elevation. As a result, inundation underestimation is inevitable.

[33] Reviewing inundation underestimation as Hurricane Hugo was nearing landfall in the previous section, one can see that such locations are all along the coasts that are subject to local water loss. When the northeasterly wind field was prevailing in the harbor before landfall, model generated inundation did not take place along the west coast of Charleston, on the west side of Scanlonville, and in some places of Sullivans Island, though the sea surface was far above land elevation.

[34] Apparently, for an estuary with a relatively wide entrance where storm surge is largely influenced by hydro-

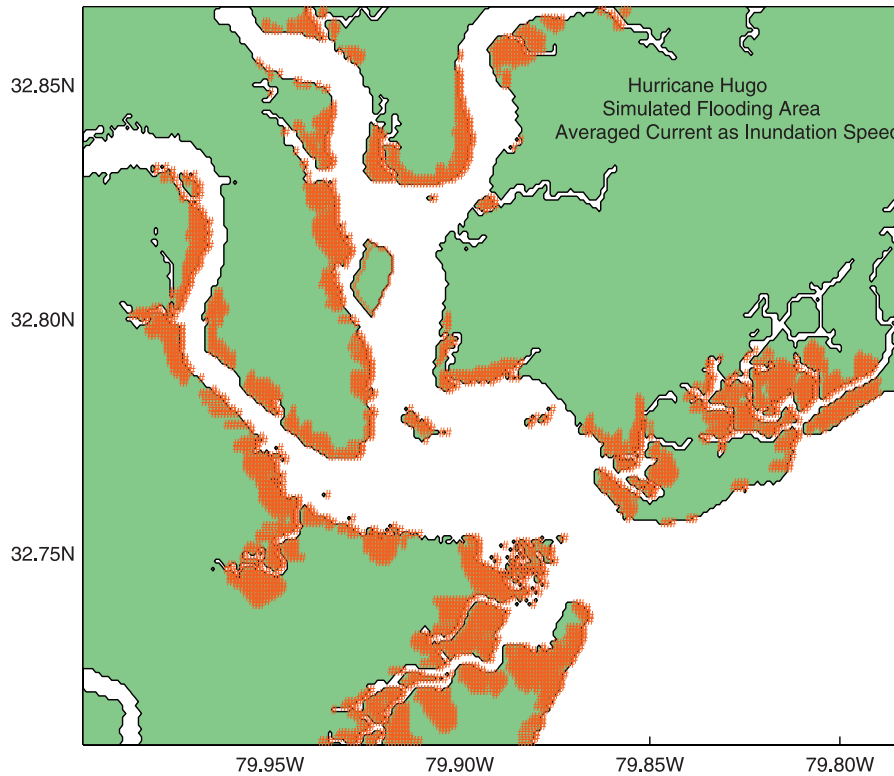


Figure 7. Model-simulated inundation of Hurricane Hugo with inundation scheme of taking vertically averaged current as the inundation speed.

dynamic environment on the shelf rather than by local wind-forcing, the inundation scheme in the XPP model may have some problems.

4.2. Other Inundation Schemes

4.2.1. Scheme Assuming Vertically Averaged Current as the Inundation Speed

[35] The HM inundation scheme assumes vertically averaged current as the inundation speed in their model. Though it has been indicated that this inundation scheme underestimates the inundation area in a closed or near closed domain [Xie *et al.*, 2004; Peng *et al.*, 2004], the scanty inundation data collected following Hurricane Emily (1993) along the CAPES coast could not demonstrate to what extent this scheme underestimates the inundation area. The well-documented inundation data incurred by Hurricane Hugo offer a good chance to further investigate this scheme.

[36] Figure 7 shows the inundation results from the HM model. The simulated inundation area is obviously much smaller than the observations in almost all regions. Sullivan's Island and the Isle of Palms, the location of Hurricane Hugo landfall, which was actually severely flooded as illustrated in Figure 6b, are apparently underestimated. Similar underestimation appears almost everywhere along the coast. This indicates that it is not appropriate to employ such an inundation scheme in the Charleston Harbor area.

4.2.2. Scheme Taking $C_t(gd)^{1/2}$ as the Inundation Speed

[37] If sea surface surpasses land elevation along the sea-land boundary, the gravity-induced pressure gradient force drives the inundation process. As the speed of the linearized gravity wave is $(gd)^{1/2}$, (g and d are, respectively, the gravitational acceleration and water depth), the inundation speed can be intuitively expressed as $C_t(gd)^{1/2}$, where $C_t \leq 1$ is a terrain-related parameter. For an ideal nonfriction smooth beach, C_t may be suggested by matching model

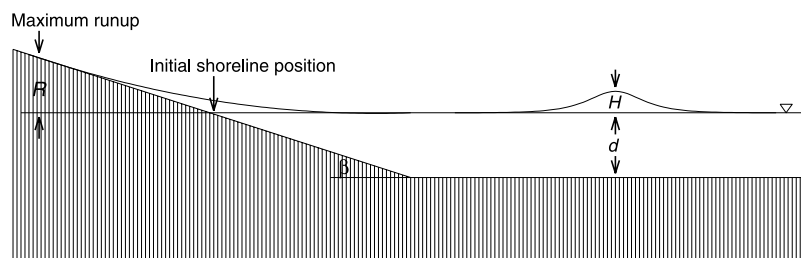


Figure 8a. A sketch of a solitary wave climbing up a sloping beach. H is the height of the solitary wave, d is the water depth on the shelf, and R is the maximum runup.

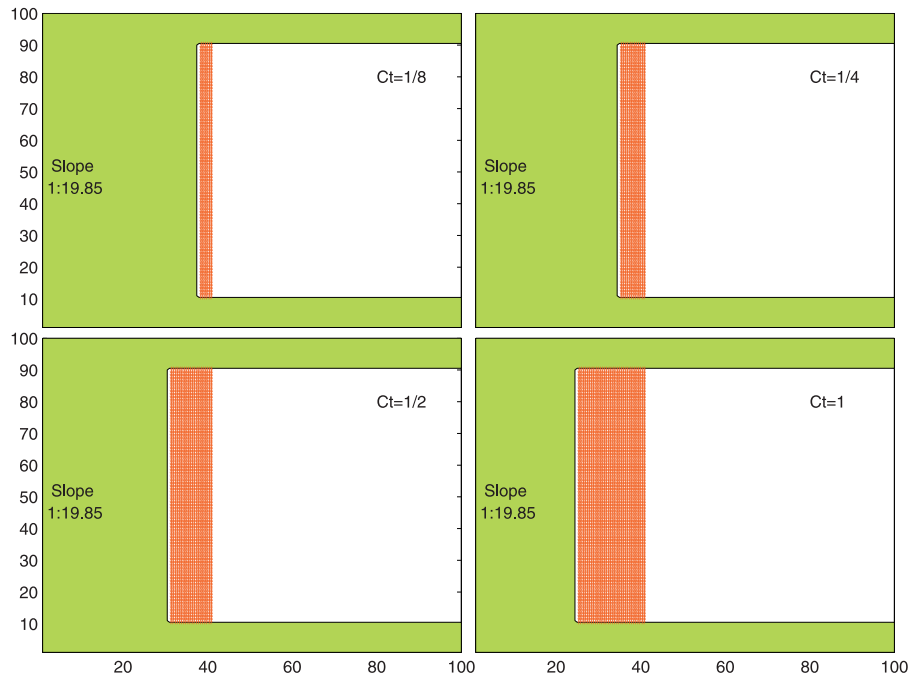


Figure 8b. The relationship between C_t and the maximum inundation in the ideal semiclosed domain, where $x = 40$ is the initial shoreline. The original water region is from $x = 41$ to $x = 100$. The grid size in y direction is 60 m. In the original water region the grid size in x direction is also 60 m, but on the original land it is 10 m. The bathymetry and land elevation profiles are sketched in Figure 8a. The beach slope is 1:19.85.

results to former laboratory experiments in the wave runup literatures [Synolakis, 1987; Kim et al., 1983; Pedersen and Gjevik, 1983].

[38] Those laboratory experiments were conducted in tanks where smooth ramp with different slope was set up

as the laboratory beach. Solitary waves were generated to study the consequent runup on the sloping beach. These long waves are similar to earthquake-induced tsunamis. Figure 8a is the sketch of a solitary wave climbing up a sloping beach. There are two crucial dimensionless varia-

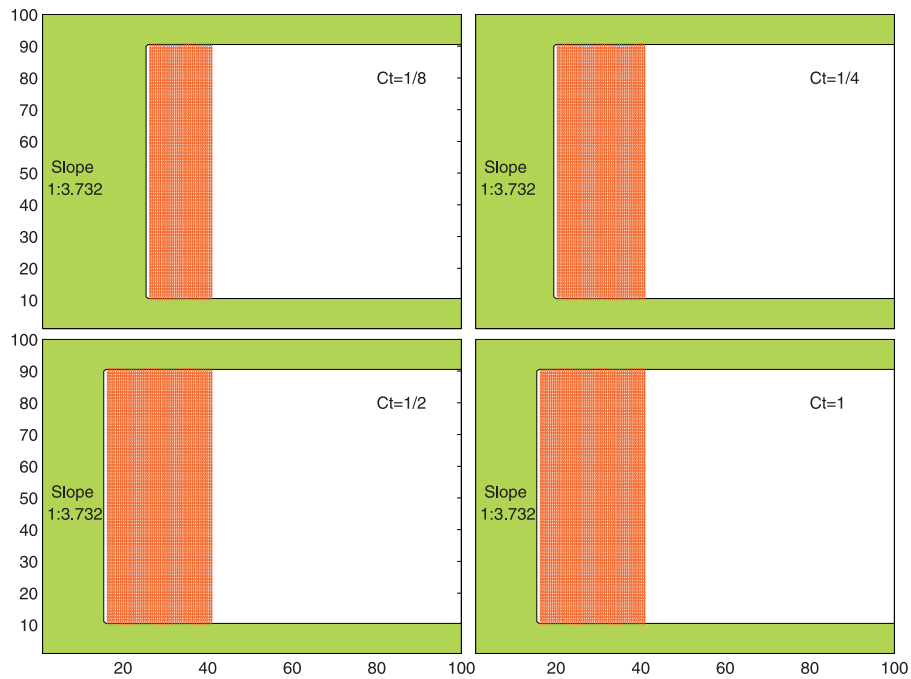


Figure 8c. The same as Figure 8b except that the grid size on the original land is 1 m and the beach slope is 1:3.732.

Table 3. Comparison of Runup From Laboratory Experiments and the Numerical Model^a

	Slope	H/d	R/d Numerical Model				
			Laboratory Data	$C_t = 1$	$C_t = 1/2$	$C_t = 1/4$	$C_t = 1/8$
Case 1	1:19.850	0.051	0.191	0.172	0.091	0.038	0.012
Case 2	1:3.732	0.050	0.173	0.135	0.129	0.096	0.082
Case 3	1:2.747	0.050	0.115	0.103	0.099	0.082	0.079
Case 4	1:1.000	0.060	0.115	0.105	0.103	0.101	0.097

^aThe laboratory data in cases 1–4 are from Synolakis [1987], Kim *et al.* [1983], Pedersen and Gjevik [1983], and Kim *et al.* [1983], respectively.

bles in the experiments. One is H/d , where H and d are respectively the solitary wave height and water depth on the shelf. The other is R/d , where R is the maximum runup on the beach. These experiment results are helpful to determine the range of C_t in various slopes and H/d conditions.

[39] An ideal semiclosed domain as in Figures 8b and 8c is used to investigate the relationship between C_t and runup (or the associated inundation) for smooth slopes. The bathymetry and land elevation profiles of the ideal domain are sketched in Figure 8a. It is a 100×100 rectangular with the original shoreline at $x = 40$ (x is the grid number from the western edge of the domain). The horizontal grid size in y direction is 60 m. In x direction the grid size is also 60 m in the original water region (x from 41 to 100). In the original land region, however, it depends on the beach slope for the purpose of clear inundation mapping. There are four

slope cases in the experiments. The slopes in cases 1–4 are respectively 1:19.85, 1:3.732, 1:2.747, and 1:1.000. In case 1, Δx on land is 10 m, but in cases 2–4 it is only 1 m owing to large slopes. The water depth on the flat shelf, d , is 60 m for all cases. The land elevation and the bathymetry between the original shoreline and the foot of the slope are determined by the beach slope as shown in Figure 8a. The land elevation on northern and southern solid boundaries is set to be 50 m to avoid unnecessary flooding on these two sides. A solitary wave, $\eta(x, t) = H \sec h^2(k(100 - x)\Delta x - kCt)$, starting from the open boundary, drives the model until its peak reaches half wavelength away from the foot of the slope. Then it propagates freely to the beach. In the above solitary wave, H is the maximum wave height, $C = \sqrt{g(d + \eta)}$, and k is $\sqrt{3H/4d^3}$.

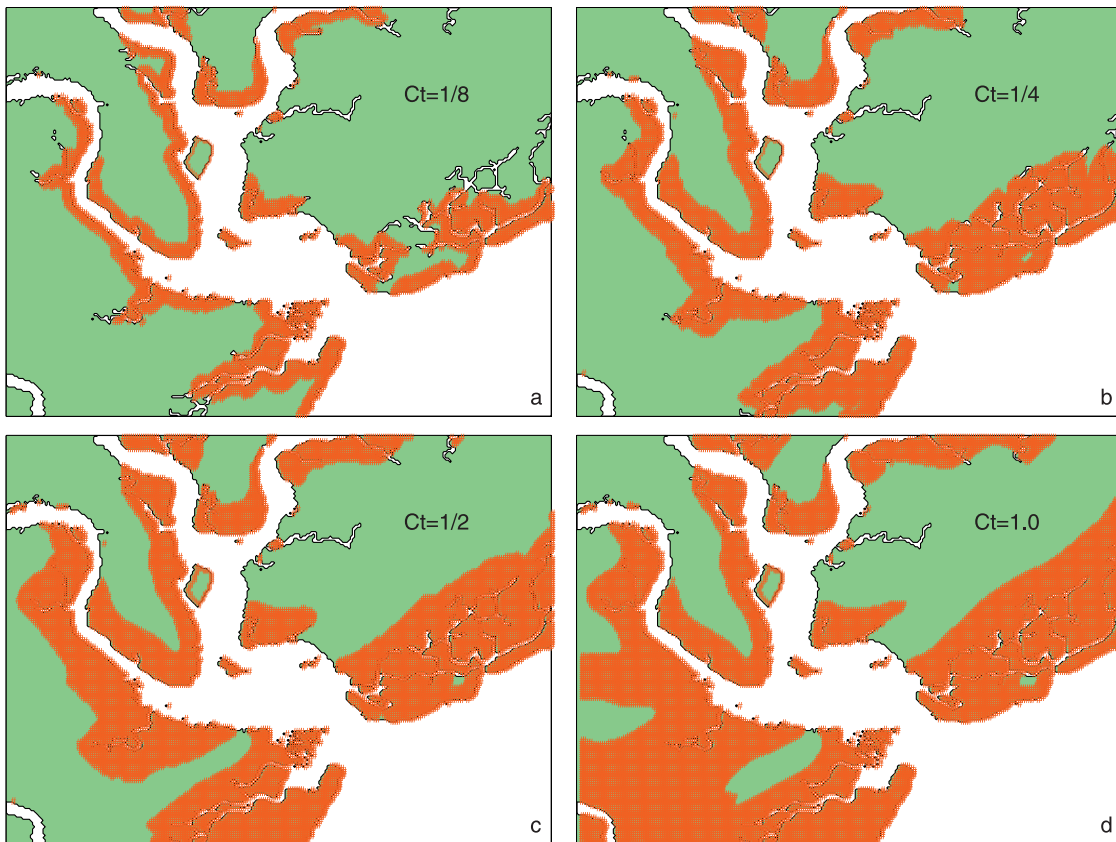


Figure 9. Model output of inundation of Hurricane Hugo with inundation scheme of taking $C_t(gd)^{1/2}$ as the inundation speed, where the terrain-related parameter C_t is set to (a) $1/8$, (b) $1/4$, (c) $1/2$, and (d) 1 , respectively.

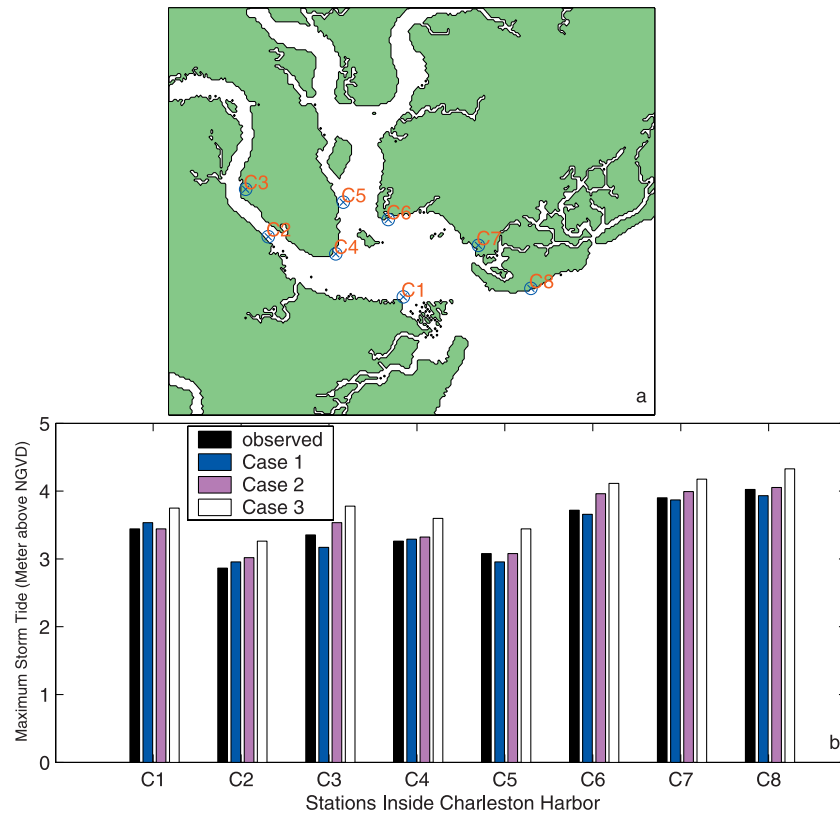


Figure 10. (a) The locations of eight storm surge stations along Charleston Harbor. (b) The observed and simulated maximum storm tide. Cases 1–3 are from taking $C(gd)^{1/2}$, surface current, and vertically averaged current as the inundation speed, respectively.

[40] The model generated maximum runups for all cases are compared with the observations in Table 3, and the associated maximum inundations of cases 1 and 2 are illustrated in Figures 8b and 8c. For case 1, the model runup agrees well with the laboratory data when C_t is 1. As C_t drops to 1/2, the runup decreases to only half of its observed data. This discrepancy increases as C_t decreases. The associated maximum inundations are shown in Figure 8b. As the slope increases to 1:3.732, the decrease of runup/inundation is not evident as C_t decreases. In fact, when C_t is 1/8, the runup and the inundation are still 3/5 of their maximum values (Figure 8c). As the slope continuously increases in cases 3 and 4, model results agree well with the observations for almost all C_t as indicated in Table 3.

[41] Apparently, it is safe to use $C_t = 1$ in the model to get a good match to the laboratory measurement in all cases (the small discrepancy is most likely due to the friction consideration in the model as will be discussed later). However, natural beach is never as smooth as the ramps used in the experiments, and vegetation and man-made structures put more friction on the coast. In real cases, the maximum runups would be smaller than in the ideal laboratory experiments. C_t , accordingly, would be smaller. The historic inundation data for Hurricane Hugo can be used to determine this terrain-related parameter in the Charleston Harbor region.

[42] How model inundation area relates to C_t in Hurricane Hugo event is illustrated in Figure 9. The results indicate

that C_t should be 1/2 to get a good match to the observation (Figure 6b). If this terrain-related parameter is appropriately set, this scheme will achieve better inundation results than choosing surface current as the inundation speed as in XPP. One can see the merits of this scheme by comparing Figure 9c ($C_t = 1/2$) with Figure 6b. The underestimation of the flooding area on the western coast of Charleston, western Scanlonville, and in some places of Sullivans Island shown in Figure 6a, no longer exists in Figure 9c. This inundation scheme appears to have great practical value in this study domain.

[43] The physical meaning of C_t was more clearly suggested by Oey [2005]. He found that the inundation speed for a long wave on a linear sloping beach depends on the friction coefficient. For a no-friction water, the inundation speed is simply $(gd)^{1/2}$, the same as long wave speed itself. When the friction coefficient increases to 10^{-2} cm/s, the inundation speed will decrease to about half of $(gd)^{1/2}$. This indicates that $C_t = 1.0$ simply means that no friction is considered. C_t will drop as friction increases. The case of $C_t = 0.5$ corresponds to a friction coefficient of 10^{-2} cm/s. As the typical value of friction coefficient of seawater is between 10^{-4} and 10^{-3} cm/s [Mellor, 1996], far less than 10^{-2} cm/s, Oey's experiments [Oey, 2005], though not declared explicitly, had, in some way, already considered the terrain-related friction. Most likely, sand, grass, trees, man-made buildings and other terrain features are the major contributors to drop C_t to 0.5 in the Charleston Harbor area.

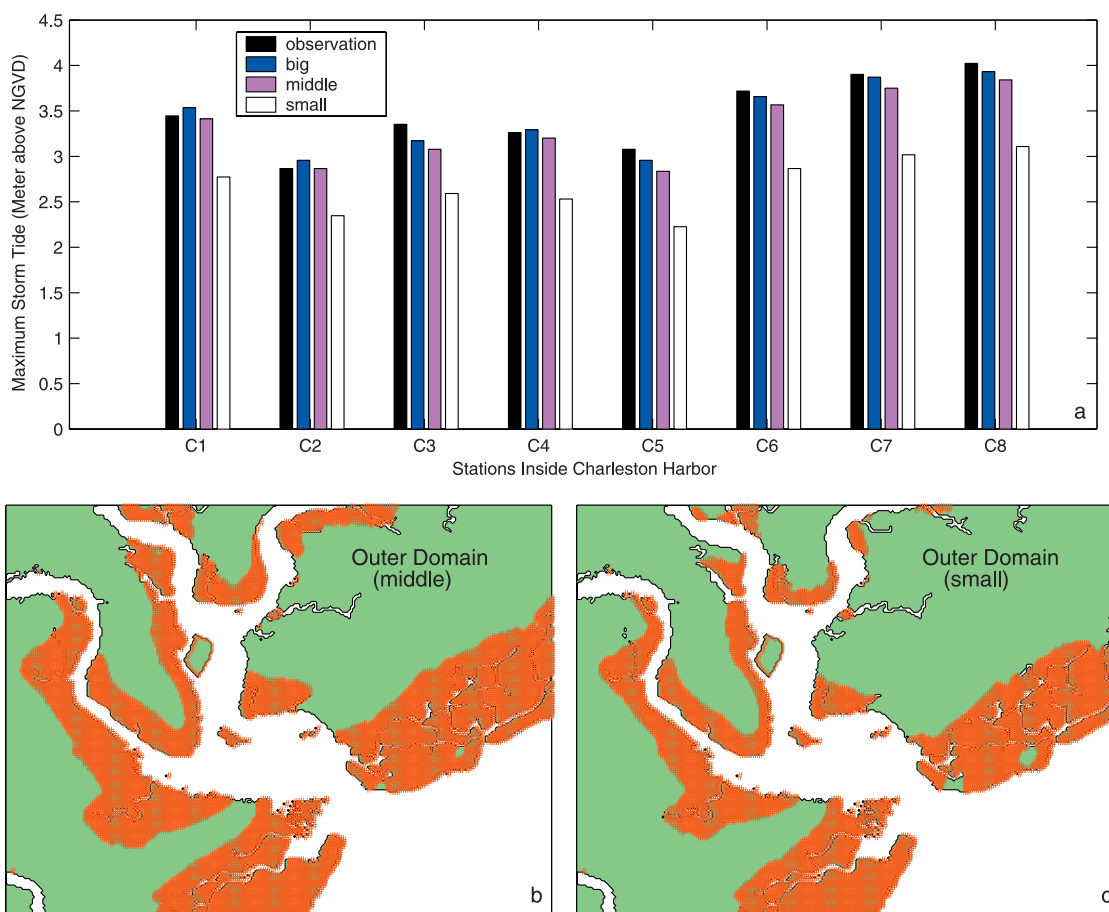


Figure 11. (a) The observed and simulated maximum storm tide at the eight stations (the locations are shown in Figure 10a). The “big,” “middle,” and “small” in the legend indicate that the corresponding model results are from taking the original (big), the middle, and the small domains as the outer domains in the model, respectively. (b) The simulated inundation result of taking the middle size domain as the outer domain. (c) The inundation result of taking the small size domain as the outer domain.

4.3. Effect of Inundation Scheme on Storm Surge

[44] The choice of inundation scheme not only determines the inundation area but also affects the storm surge along the coast. To assess the variation of storm surge with different inundation schemes, and to evaluate the difference between these model results and the measurement values, eight stations were chosen around Charleston Harbor for comparison as shown in Figure 10a. The measured and three simulated maximum storm tides from model runs with different inundation schemes are shown in Figure 10b. Cases 1–3 in Figure 10 are the results respectively by utilizing $C_t (gd)^{1/2}$ ($C_t = 0.5$), the surface current, and the vertically averaged current as the inundation speed.

[45] The simulation results of case 1 agree well with the observations. Generally, the maximum storm tide difference between case 1 and observations is less than 15 cm at most of the stations, except for station 3 where the difference is 20 cm. Case 2 also shows good comparison with observations, except at C3 and C6, where the difference between model results and measurement is evident. This is because wind direction (and the subsequent surface current) at both stations was pointing away from the coast when Hurricane Hugo was approaching (see Figure 6a for the simulated

inundation in this case). As inundation is hampered by the second inundation criterion in the model, the corresponding storm surge at the two locations is higher owing to water piling-up process against the “solid” coast. Case 3 overestimates the storm surge at every station. This is because this inundation scheme underestimates the extent of inundation essentially everywhere (see Figure 7 for the inundation of case 3).

[46] Generally, embedding different inundation schemes in the model not only results in different inundation area, but also induces a difference in storm surge calculation. Inundation underestimation can produce an overestimation of storm surge in the corresponding locations, and vice versa. The storm surge difference among all the inundation schemes, in this specific hurricane case, can reach up to half a meter at some locations, as shown in Figure 10.

5. Size of the Outer Zone and the Results

[47] The size of the outer domain is important for the model output. As the radius of maximum wind of typical Category 2 and 3 hurricanes is on average about 50 km as they approach the coast [Hsu and Yan, 1998], a region larger

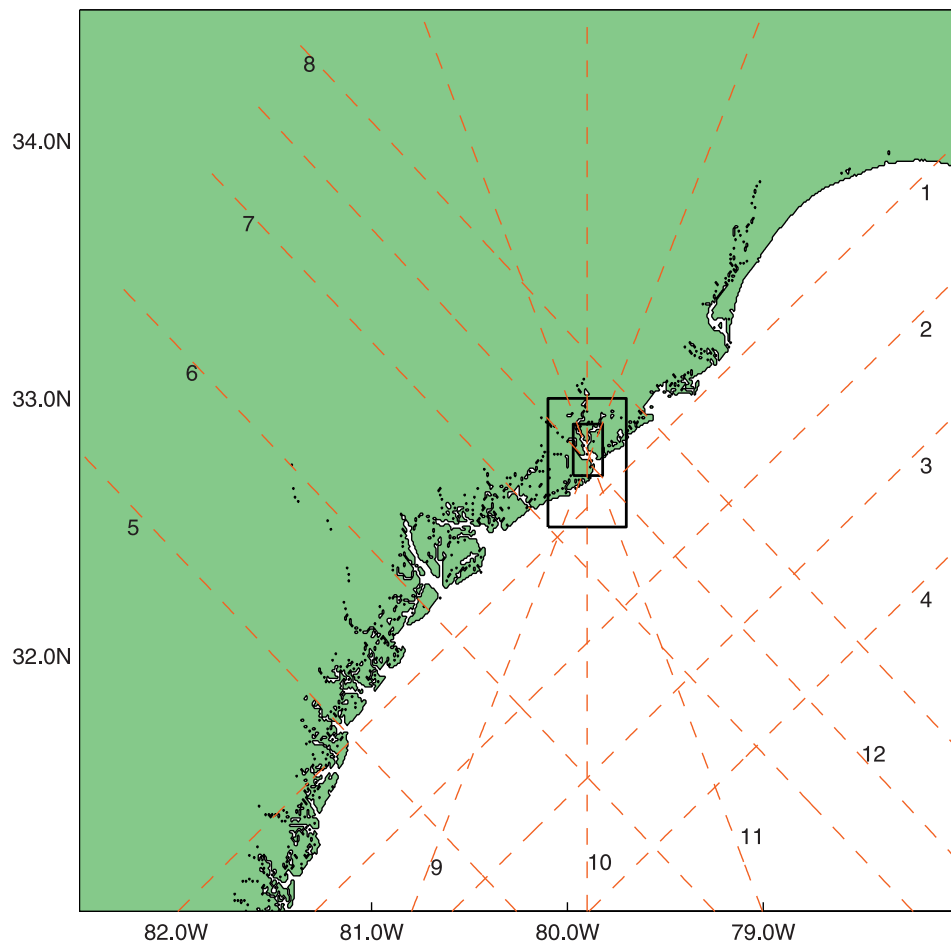


Figure 12. The hypothetical hurricanes with track numbers 1, 2, 3, and 4 as group 1, which parallels the coast; track numbers 5, 6, 7, and 8 as group 2, which is perpendicular to the coast; and track numbers 9, 10, 11, and 12 as group 3, which makes landfall at downtown Charleston.

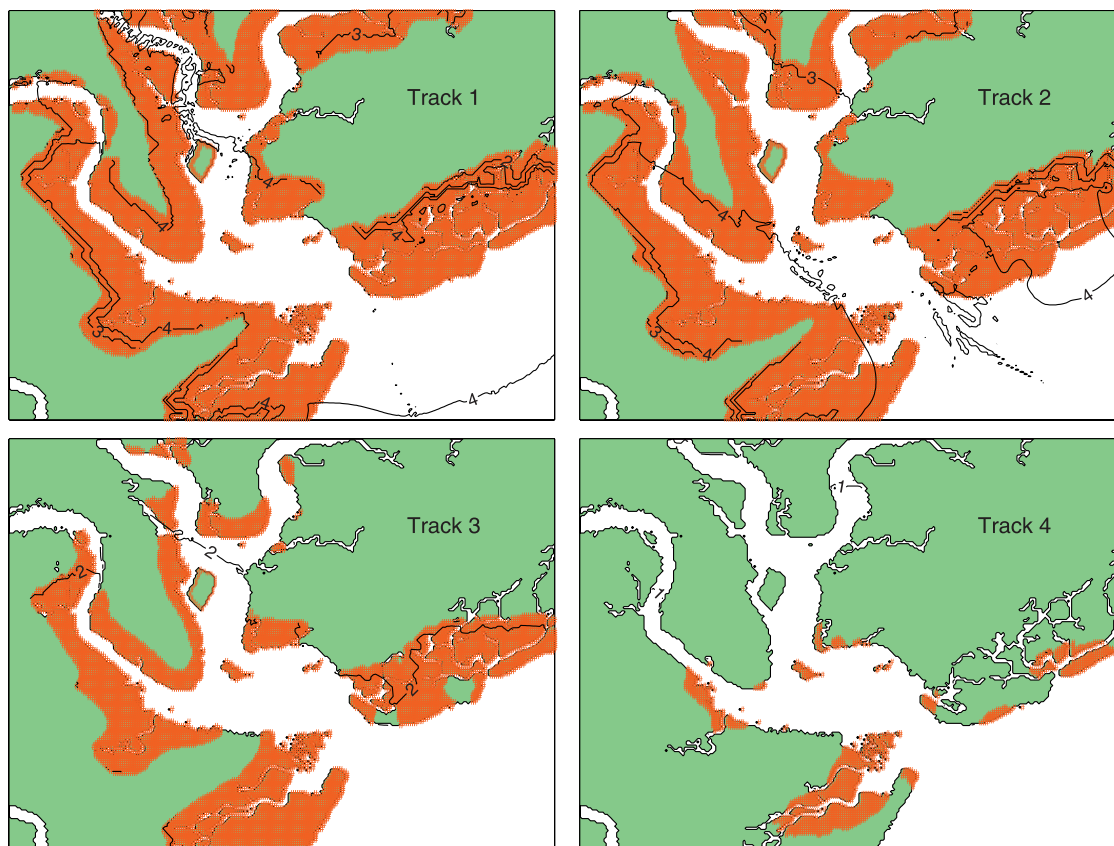
than 100 km in diameter around the hurricane center may be significantly affected. Thus, given the spatial extent of Charleston Harbor, the outer model domain must be far larger than the harbor's size. On the other hand, computer resources are not unlimited, and too much enlarging of the outer domain consumes unnecessary computer resources. So, the reasonable size for the outer domain needs to be carefully considered.

[48] To evaluate the effect of different outer domain size on simulation results, the original outer domain was decreased to 78.5–82.5°W, 31.5–34.5°N for a middle size case, and to 79.0–82.5°W, 32.0–34.5°N for a small size case (figures are not shown for these boundaries). So, the southern and eastern boundaries of the outer zone were cropped 0.5° and 1.0°, respectively, for these two cases. The original domain is named “big size case” for comparison. The grid sizes are the same as those in section 2.

[49] The simulated maximum storm tide at the eight stations of Figure 10a and the inundation area in the Charleston Harbor region are shown in Figure 11. The inundation scheme of using $C_t (gd)^{1/2}$ ($C_t = 0.5$) is applied for all cases. For comparison, the storm tides of observation and of the “big size case” are also shown in Figure 11.

[50] The results indicate that for the “middle size case” the maximum storm tide at these stations decreases modestly compared with the “big size case.” The decrease is less than 10 cm at all stations. The simulated inundation is correspondingly shrunk, but the difference is small (see Figure 11b and Figure 9c for comparison). Simulated storm tide and inundation area for the “small size case” decrease evidently. Compared with the original case, the difference of the maximum storm tide is typically around 50 cm. At some stations, such as C7 and C8 the difference is over 70 cm. As a result, underestimation of inundation area around Charleston Harbor is evident as shown in Figure 11c (also see Figure 9c for comparison). For instance, the simulated inundation is apparently smaller on both sides of Charleston Downtown, the south coast of Daniel Island, western Scanlonville, and the coastal region between James Island and Morris Island.

[51] The outer domain was also enlarged in the study (not shown) to see how it affects the model results. In the experiment, an additional 0.5 degree was added to the northern, eastern, and southern boundaries. The results have almost no difference from the original outer domain case. The difference of the maximum storm surge, for instance, is less than 1 cm at all stations.



Figures 13a. The simulated maximum storm surge and inundation distributions induced by the hypothetical hurricanes with central pressure of 940 mbar and radius of maximum wind (RMW) of 50 km for group 1. The translation speed is 36.5 km/h. Storm surge is in meters.

[52] As indicated above, choosing a different size for the outer zone will yield different results. A smaller zone will underestimate both storm surge and inundation. As the size of the zone enlarges, that misrepresentation will taper off. In Hurricane Hugo's case, the difference is essentially insignificant between the "middle case" and the original case. In this regard, choosing the original outer zone for the model run is reasonable. Of course, this outer domain is not necessarily the best one.

6. Hurricanes With Different Tracks

[53] If other hurricane features such as RMW and central pressure are assumed constant, hurricane track will determine the extent of storm surge and inundation. A hurricane may produce very different inundation and storm surge with just a slight track change. This will be illustrated in this section.

[54] To consider the effect of hurricane tracks on storm surge and inundation, 12 tracks were deployed as in Figure 12 (with the hurricanes moving from lower latitude). The central pressure and RMW are 940 mbar and 50 km, respectively, for all hypothetical hurricanes, with 36.5 km/h as the translation speed, which is the same speed when Hurricane Hugo was approaching Charleston Harbor. This group of experiments is named Ex 1 to differ from the others in the next section. The central pressure and RMW are chosen in keeping with *Hsu and Yan* [1998] for

their statistical relationship. Tracks 1–4 (group 1) parallel the coast and are 40 km apart. Tracks 5–8 (group 2) are perpendicular to the coast and are 60 km apart. Tracks 9–12 (group 3) pass through (i.e., make landfall at) Charleston and vary 22.5° apart in direction. Figures 13a–13c shows the storm surges and the associated inundations in Charleston Harbor produced by all these hypothetical hurricanes.

6.1. Group 1

[55] The simulated results show that track 1, which passes 20 km away from the coast of Charleston, can generate 4 m storm surge in almost all coastal regions around the harbor. Both the storm surge and inundation are the most severe among all the cases in this group (see Figure 13a). The inundated area is over 100 km² (see Table 4). Track 2, which is 60 km offshore, generates storm surges that are about 0.5 m smaller than those produced by track 1. The associated inundation area has no apparent decrease. As the eye of the hurricane is displaced an additional 40 km further seaward to track 3, both the storm surge and inundation decrease dramatically. The storm surge in most of the harbor area decreases to less than 3 m, and the inundation area shrinks to about 50 km² as shown in Figure 13a and Table 4. Finally, when the hurricane moves to track 4, the storm surge is less than 2 m in almost all areas. Light inundation exists only along the coast of Sullivan's Island, Scanlonville, James Island, and Morris Island, and there is no flooding in the Charleston Peninsula or the other subregions north of it.

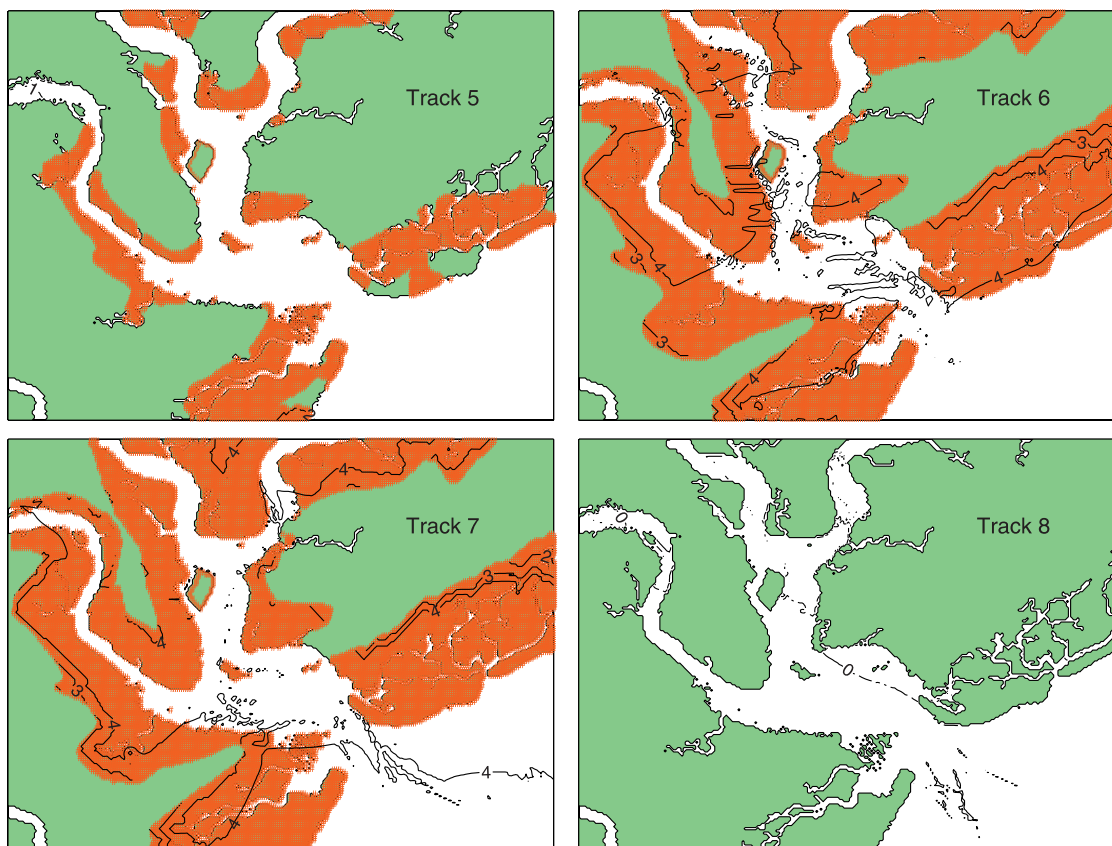


Figure 13b. The simulated maximum storm surge and inundation distributions induced by the hypothetical hurricanes with central pressure of 940 mbar and radius of maximum wind (RMW) of 50 km for group 2. The translation speed is 36.5 km/h. Storm surge is in meters.

[56] The simulation results indicate that, for hurricanes whose paths are parallel to the coast, severe storm surge and inundation in the Charleston Harbor area are produced by those hurricanes that are within 60 km from the coast. The closer to the coast the track is, the more severe the storm surge and inundation will be.

6.2. Group 2

[57] As the distance of track 5 is more than 150 km away from Charleston, the associated storm surge and inundation are moderate. In this case, the maximum storm surge is 2 m along the southern coast of Morris Island, and much smaller inside the harbor (Figure 13b). As the track moves 60 km closer to Charleston, the hydrodynamic effect of the hurricane in the harbor becomes stronger. Track 6 results in a typical 4 m surge in most coastal regions. The inundation (129 km²) covers most of the harbor coast as shown in Figure 13b. As the hurricane moves to track 7, only 30 km to the southwest of the harbor mouth, the storm surge increases approximately 0.5 m in most areas while slight decrease occurs for the inundation area (see Table 4). When the hurricane moves to the other side of the harbor to track 8, the storm surge decreases to less than 1m in all regions, and no inundation takes place across the entire region. This is because, moving along this track from southeast to northwest, the anticlockwise wind results in water loss in Charleston Harbor, rather than gaining water.

[58] For the four hurricanes with tracks perpendicular to the coast, track 7 is the one that produces the most severe storm surge, and track 6 induces the largest inundation area. The maximal cases for both surge and inundation for all perpendicular hurricanes (not limited to the four assumed ones) could be along a swath somewhere between tracks 6 and 7. Of course, the track producing the greatest surge, and the one producing the largest extent of inundation, may not be the same track.

[59] Attention should be paid to the dynamical response of the harbor if the hurricane's parallel track is located to the northeast side of the mouth of Charleston Harbor (track 8). In such a case, storm surge and inundation are no longer a threat to the harbor. When the track distance is only 30 km away from Charleston, there is no inundation at all across the entire Charleston Harbor region, and the surge is practically negligible. In fact, in this case, the maximum sea surface elevation remains negative for most regions in the vicinity of the harbor.

6.3. Group 3

[60] Tracks 9 and 10 produce similar surge height and inundation area. The storm-induced maximum surge ranges from 4.5 m to 5.5 m in coastal areas, and lateral inundation is very severe (about 120 km² for both tracks). Most land is flooded at Charleston, and the inundation along the other coastal subregions is also intensive (see Figure 13c). As the track turns 22.5° anticlockwise from track 10 to 11, both

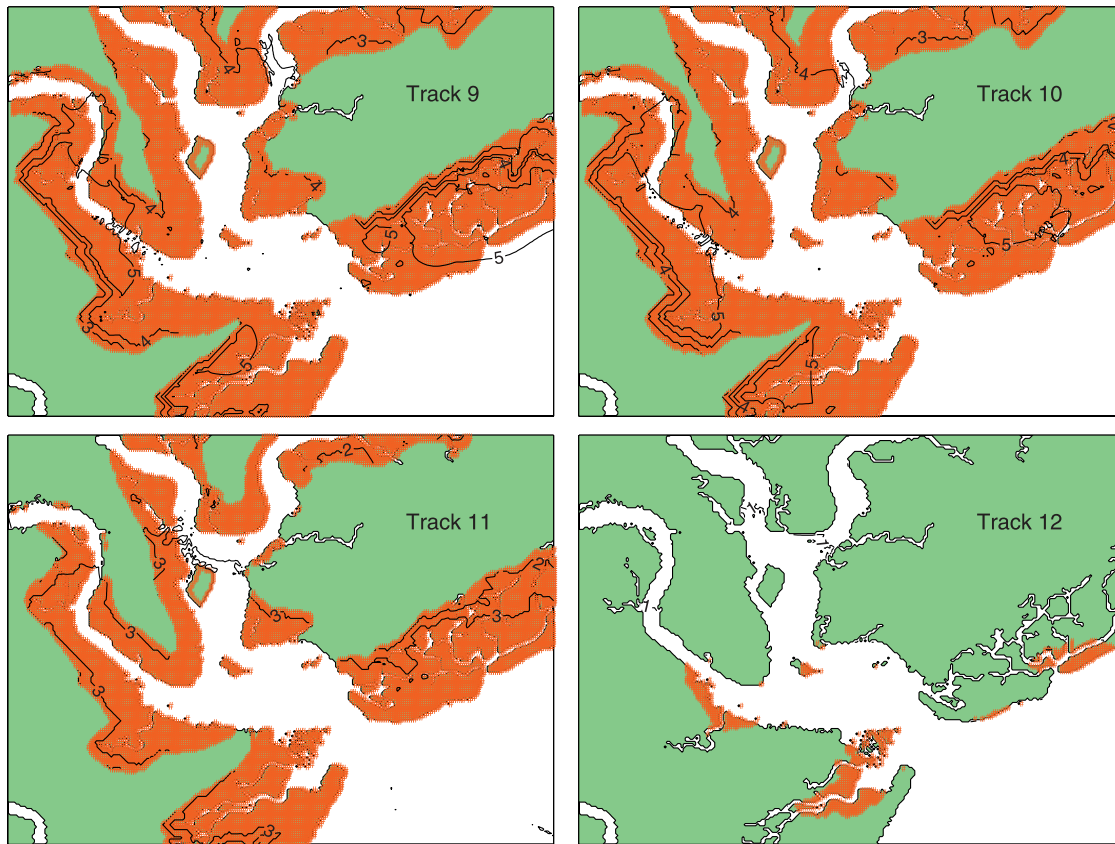


Figure 13c. The simulated maximum storm surge and inundation distributions induced by the hypothetical hurricanes with central pressure of 940 mbar and radius of maximum wind (RMW) of 50 km for group 3. The translation speed is 36.5 km/h. Storm surge is in meters.

surge and inundation decrease. In this case, the typical maximum storm surge decreases to about 3.5 m in the harbor area, and the areal inundation lessens to a moderate extent (90 km²) as shown in Figure 13c. Track 12 is a special one. It not only makes landfall at Charleston, as every track in group 3, but is also perpendicular to the coast, as in group 2. The storm surge and inundation in this case are generally negligible. The storm surge is less than 2.5 m

in the entire harbor region, and the inundation area shrinks dramatically compared with the other tracks in group 3.

[61] For hurricanes that make landfall at Charleston, the most severe inundation is produced by the track that comes from a direction between south and southwest. The highest storm surge is produced by the one that parallels (or nearly parallels) the coast. This conclusion is deduced from the simulation results for groups 1 and 3. As the track turns

Table 4. Overall Maximum Storm Surge and Inundation Area in All Cases^a

Track	Ex 1 (940 mbar, 50 km)		Ex 2 (950 mbar, 50 km)		Ex 3 (930 mbar, 50 km)		Ex 4 (940 mbar, 30 km)		Ex 5 (940 mbar, 70 km)		Ex 6 (940 mbar, 50 km)	
	SS	IA										
1	5.14	105.73	4.89	104.85	6.31	128.07	4.40	60.16	5.43	129.68	4.96	144.20
2	4.76	105.04	4.53	91.45	5.93	128.60	3.02	40.01	5.19	137.18	4.77	144.98
3	2.99	59.70	2.62	32.21	3.86	91.67	2.08	1.60	4.32	114.42	3.31	103.17
4	2.09	11.66	1.52	0.01	2.41	34.34	1.30	0.00	2.86	72.21	2.23	48.40
5	2.36	44.92	2.07	27.21	2.81	86.38	0.82	0.00	3.81	120.31	2.46	53.41
6	4.53	129.45	4.33	122.94	5.50	153.41	2.10	30.17	6.04	166.62	4.18	143.57
7	5.03	127.15	4.96	123.79	6.02	145.34	5.10	101.01	4.26	114.58	5.01	155.02
8	0.69	0.00	0.47	0.00	0.79	0.00	0.49	0.00	0.66	0.00	0.95	0.00
9	5.56	119.78	5.11	117.95	6.64	139.59	4.91	79.77	6.03	134.86	5.43	164.97
10	5.35	121.13	4.95	112.36	6.52	140.24	5.06	87.26	5.54	132.87	5.75	167.26
11	4.37	90.16	3.72	65.89	4.95	109.63	3.71	57.75	4.43	98.28	4.40	128.07
12	2.31	7.09	2.26	1.72	2.61	18.70	2.27	3.09	2.32	8.52	2.64	29.51

^aExs 1–5 are fast hurricanes with translation speed at 36.5 km/h, and Ex 6 is a slow hurricane with translation speed of 18.25 km/h. Each hurricane’s central pressure and radius of maximum wind (RMW) are given in the table. The maximum storm surge (SS) and inundation area (IA) are in m and km², respectively.

perpendicular to the coast, the extents of both surge and inundation dramatically dwindle.

7. Conclusions and Discussion

[62] The *Xie et al.* [2004] storm surge and inundation model was configured in Charleston Harbor and its adjacent coastal region to investigate the harbor's response to hurricanes. Hurricane Hugo's induced storm surge and inundation along with its track and pressure data were well documented, which are used in this paper to validate and improve the previously developed surge and inundation model.

[63] The comparison of model results with observations indicates that, in this study domain, taking the calculated surface current as the speed of inundation is not the best inundation scheme, though it works well for a closed or near closed domain as demonstrated in previous studies [*Xie et al.*, 2004; *Peng et al.*, 2004]. Such inundation schemes underestimate inundation area in places where the local wind induces local water loss. For a small coastal region like Charleston Harbor (compared with the spatial scale of typical hurricanes), its open feature suggests that the coastal surge and the consequent inundation are generally determined by the gravity waves that are generated on the continental shelf, not by the local wind-forcing.

[64] Assuming vertically averaged current as the inundation speed produces even less accurate results. Though it was claimed to perform well for the surge and inundation forecast along the Australian coast [*Hubbert and McInnes*, 1999], it does not work well for Charleston Harbor. Also, such an inundation scheme consistently underestimates the inundation area in a closed or near closed domain as demonstrated in previous studies [*Xie et al.*, 2004; *Peng et al.*, 2004]. Another option is to assume $C_t(gd)^{1/2}$ as the inundation speed. This assumption leads to more accurate model results, given that the terrain-related parameter C_t is accurately chosen. For an ideal no-friction sloping beach, $C_t = 1$ seems consistently reliable. In real cases, however, historic storm surge and inundation records along with the associated meteorological data are necessary to choose C_t in the concerned region. If the necessary data have not been well documented, or the territory is virgin, this method may not be employed.

[65] Different inundation schemes not only produce different inundation but also alter the storm surge height along the coast. For a scheme that underestimates inundation extent, such as taking the vertically averaged current as the inundation speed, or taking the surface current as an alternative (though the extent of inundation underestimation of the latter is much less than the former), the storm surge will be overestimated along the original sea-land boundary. In most cases, the surge overestimation is moderate. However, for a Category 4 hurricane like Hurricane Hugo, the overestimation of storm surge can be up to half a meter at some coastal locations if the vertically averaged current is taken as the inundation speed.

[66] Appropriate nesting domains are also important for obtaining reliable model results. In a small study domain like Charleston Harbor, whose spatial scale is far less than that of a typical hurricane, the appropriate choice for the outer domain is pivotal. It is not advisable to unlimitedly

enlarge the outer domain to capture all hydrodynamic information of a passing hurricane when a smaller domain suffices for the same purpose. On the other hand, if the outer domain is shrunk to the extent that the domain can no longer capture the necessary information, the simulated storm surge and inundation will be underestimated. Thus the question of how to deploy the nesting domain depends on the spatial scale of the specific hurricane. In the case of Hurricane Hugo, shrinking the original outer domain to 79.0–82.5°W, 32.0–34.5°N will apparently underestimate the surge and inundation in Charleston Harbor.

[67] Hurricane-induced storm surge and inundation are very sensitive to storm tracks. Twelve hurricanes with different tracks were invoked to investigate how Charleston Harbor might respond to tracks that parallel, or are perpendicular to the coastline, or landfall at Charleston at an angle. If the RMW and central pressure are fixed respectively to 50 km and 940 mbar as in Ex 1 for a typical Category 4 hurricane, for those that parallel the coast, the most severe storm surge and inundation are produced by tracks that are less than 60 km away from the coast. For the group of hurricanes that are perpendicular to the coast, track 7 produces the highest storm surge while track 6 induces the most severe inundation. As the track moves to the right of the harbor mouth, both surge and inundation decrease sharply. For the group of hurricanes that makes landfall at Charleston, those coming from due south or with a slight offset to the west (like tracks 9 and 10) bring severe storm surge and inundation in Charleston Harbor. However, as the hurricane direction tilts counterclockwise from south to southeast (almost perpendicular to the coast as in the case of track 12), both surge and inundation decrease dramatically.

[68] Even though the central pressure and radius of maximum wind in Ex 1 are typical for Category 4 hurricanes, the values in real hurricanes may vary greatly [*Hsu and Yan*, 1998]. To consider more storm surge and inundation responses to different central pressure and RMW, four additional experiments are contrived for discussion: Ex 2, 950 mbar, 50 km; Ex 3, 930 mbar, 50 km; Ex 4, 940 mbar, 30 km; Ex 5, 940 mbar, 70 km. As hurricane translation speed may also affect the storm surge height and inundation area [*Peng et al.*, 2004], in another additional experiment, Ex 6, the hurricane translation speed is set to 18.25 km/h, or half as in Ex 1. The other parameters in Ex 6 are the same as in Ex 1. The results show the sensitivity of the surge and inundation to the changes of central pressure, RMW, and translation speed.

[69] The storm surge and inundation distributions for Exs 2–6 are not shown in this paper, but the overall maximum storm surge in the entire region and the inundation area of the experiments are shown in Table 4. The details of these results are not discussed. Only the general conclusions are briefly given.

[70] As the hurricane's central pressure decreases from 950 to 930 mbar, both storm surge and inundation increase. The extent of increase for storm surge or inundation is nonlinear. The increase, with central pressure dropping from 940 to 930 mbar, generally is much greater than when the pressure decreases from 950 to 940 mbar. This is especially true for the storm surge height whose average increase for all tracks in the respective pressure-decreasing sections is

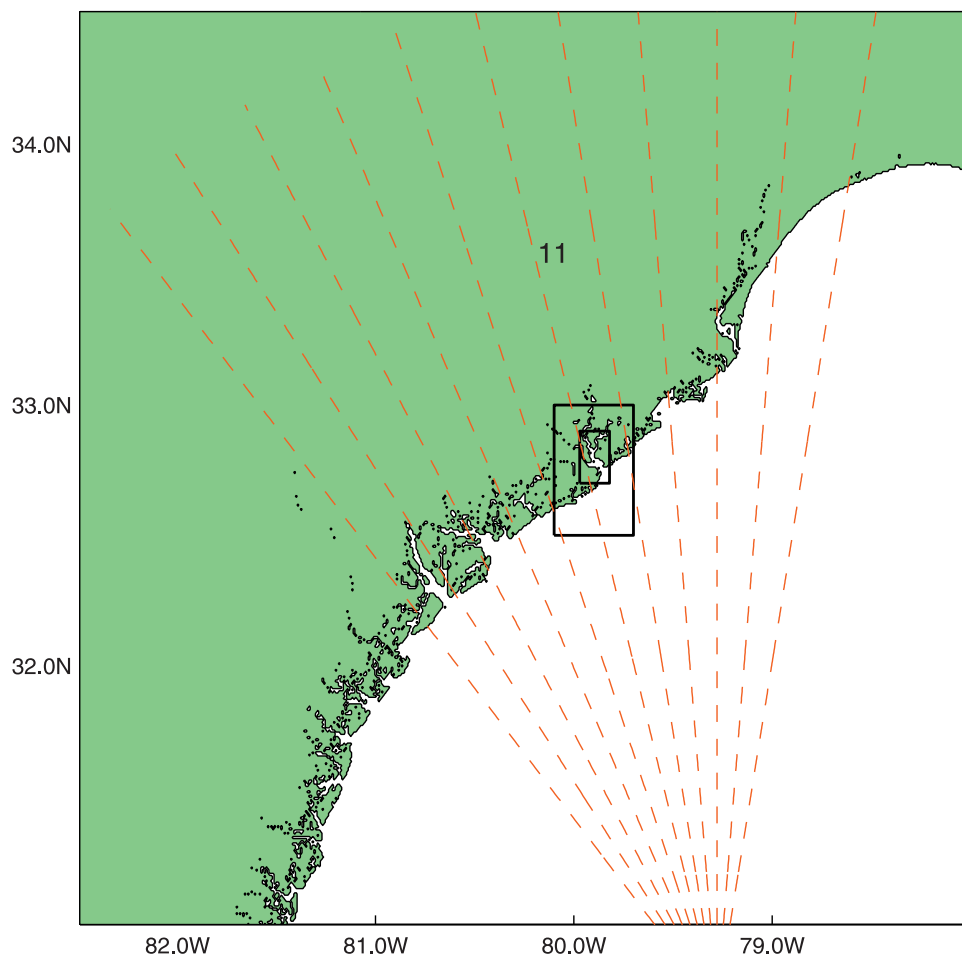


Figure 14a. All possible tracks with track 11 as the most possible one.

0.76 and 0.31 m. This indicates that the same decrease of central pressure can bring more increase in storm surge and inundation when the pressure value is lower.

[71] Increase of RMW may also increase storm surge and inundation. If we consider an ultimate large region as the target, for example, the outer domain in Figure 2, the overall maximum storm surge and inundation of the entire coastal region will invariably increase. However, as our final target region is Charleston Harbor, the inner domain of our nesting system, how the harbor responds to the variation of RMW depends on the orientation of the track and the value of RMW. For hurricanes whose tracks parallel to the coast, RMW increases always lead to the corresponding increases of surge and inundation in the harbor region. For those that are perpendicular to the coast, the above statement is also true only if the track keeps a distance from the harbor. This distance, as the results of Exs 1, 4, and 5 indicate, is very close to the hurricane's characteristic scale, that is, its RMW. When the hurricane track is far away from the harbor, tracks 5 and 6 for instance, the increase of RMW from 30 km to 50 km or from 50 km to 70 km all makes storm surge and inundation more severe. The results for track 7 are different. The overall maximum storm surge takes place when RMW is 30 km (see Table 4), rather than 50 or 70 km. This is because, as mentioned before, track 7 is

only 30 km away from Charleston. When hurricane's RMW is larger than this distance, the severity of storm surge and inundation may decrease. For the hurricanes that make landfall at Charleston, the increase of RMW may always lead to increases in surge and inundation.

[72] It is hard to comment on which factor more severely induces storm surge or inundation in the harbor, the increase of RMW or the decrease of central pressure. Generally, as the results of Exs 1–6 indicate, when a track is close to the harbor or making landfall at it, decreasing central pressure more effectively increases the storm surge and inundation in the region. Otherwise, when the track is far away from the harbor, such as tracks 3–6, enlarging RMW may more intensely increase the strength of surge and inundation (see Table 4 for comparison). One has to bear in mind that only limited tracks are used in the study. Discretion is needed to determine if a real hurricane, with its own specific track, should be considered as a close or far one when its RMW is given.

[73] Slower hurricanes may invariably induce more inundation, but may not certainly induce more storm surge. If and how much a slower hurricane can make different surge height from a faster hurricane depends on the faster's moving speed and the distance of the track from the harbor. If the faster one, considering its distance and orientation

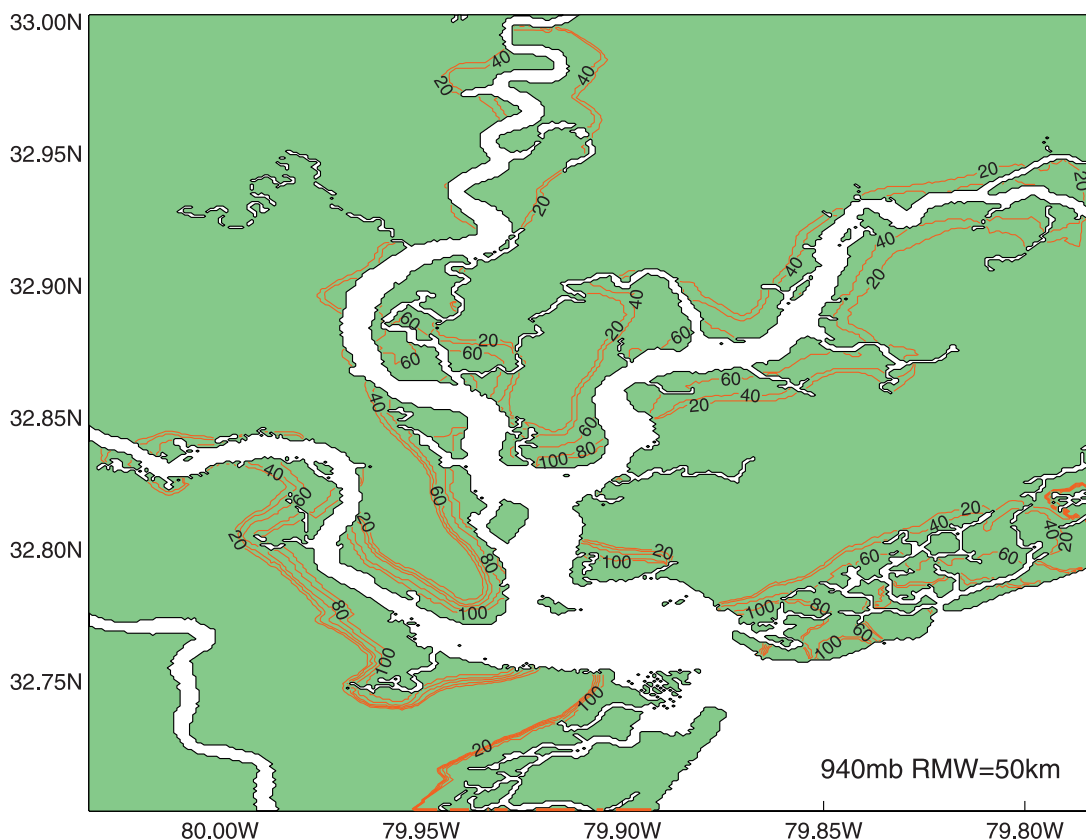


Figure 14b. The probability of being inundated in Charleston Harbor and its adjacent coast with the possible tracks shown in Figure 14a.

relative to the harbor, has already made the surge height fully developed (or matured), decreasing its translation speed will make no difference. In some cases, the overall maximum storm surge will go down rather than up (see Table 4). This is largely because of the feedback of the inundation to storm surge as illustrated in section 4. For example, tracks 3 and 4 are obviously not fully developed with its assumed central pressure (940 mbar), RMW (50 km) and the fast moving speed (36.5 km/h), for the storm surge increases when its moving speed dwindles to half of its original value as indicated in Table 4. For most other tracks, the original fast moving hurricanes seem already “matured” or near “matured” (see Ex 1 and Ex 6 in Table 4 for comparison). This means, in such cases, decreasing hurricane’s translation speed can no longer increase the maximum storm surge.

[74] Let us review Hurricane Hugo and its induced storm surge and inundation with all previous discussions in mind. The track of Hugo ran somewhere between tracks 11 and 12, as assumed in Figure 12. If its track had tilted clockwise to some extent, like tracks 10 or 9, the already historically recorded storm surge and inundation would have been more severe. On the basis of Table 4, the maximum storm surge would have been at least 1.0 m higher than its record, and the inundation area would be at least 30% more. If Hugo’s central pressure had averagely decreased 10 mbar along its track before landfall, the storm surge would have increased at least 0.5 m, and more severe inundation would have occurred correspondingly. As a quasi-landfall hurricane (its

landfall location was not exactly at the center of Charleston Harbor), if Hugo’s RMW had been moderately larger than its real value, the corresponding variations in storm surge and inundation would have been smaller comparing to effects of the other two mentioned factors. Translation speed is another potential hurricane feature that can change storm surge and inundation area. However, in Hurricane Hugo’s case, its original speed (36.5 km/h before landfall) has already made it fully developed, or very close to it, so as to the maximum storm surge, slowing down its moving speed would not have made much difference. Of course, a slower translation speed would have certainly made Hugo-produced inundation more severe.

[75] Listed above are the possible contributors that would have led to more severe storm surge and inundation for Hurricane Hugo. Reversing each factor would have lessened the disasters. As another example to show the importance of the hurricane tracks to surge and inundation, Hugo’s original track again is rotated, but this time counterclockwise, to an orientation that is perpendicular to the coast, with its landfall location unchanged. This track is almost the same as track 8 in group 2 though the distance is about 15 km closer to the harbor. If Hugo had approached Charleston Harbor along this track, its induced storm surge and inundation, if any, would have been dramatically dwindled.

[76] The combination effect of the hurricane’s intensity, RMW, track, landfall location and translation speed on storm surge and inundation was studied by [Jelesnianski,

1972; Jelesnianski et al., 1984; Jelesnianski et al., 1992], and conclusions similar to this paper were made on the basis of their hypothetical hurricanes. However, the accuracy of the storm surge and inundation of the SLOSH model may be inferior to the XPP for the following reasons: (1) SLOSH, a 2-D model which ignores advective terms in the equations, may lead to storm surge underestimation [Pietrafesa et al., 1986] compared with a 3-D model. (2) B-grid scheme is used in SLOSH though C-grid is generally preferred in the numerical calculation of water motion equations [Jelesnianski et al., 1992], and the advantage of using C-grid (as in XPP) is more apparent when a movable sea-land boundary problem is handled. This is the reason why so many artificial assumptions have to be made in SLOSH when flooding or exhausting is being processed near sea-land borders. (3) The topography input of SLOSH is based on the USGS 7.5 min DEM database, and this, with no doubt, will lead to inaccuracy when the details of storm surge and inundation are required for the inner domain of Charleston Harbor, where high bathymetry and land relief resolution is needed.

[77] Forecast of hurricane produced storm surge and inundation is a challenge in Charleston Harbor. A real hurricane may not approach the harbor on any of the hypothetical tracks that were deployed in this study. Moreover, its RMW and central pressure at a time may vary greatly from the assumptions under which all the simulations were conducted. No simple conclusion about potential surge and inundation should be made before a model simulation is completed with accurate input of observed RMW, central pressure, orientation of the track and other crucial information like hurricane's translation speed.

[78] Furthermore, all the study results in this paper are valuable only if the approaching hurricane's features are accurately forecast. This may happen when the hurricane is very close to the coast. If the hurricane's eye is still far from the coast with great uncertainty as to where it will move next, a probability forecast is more useful and has greater value for evacuation warnings. For example, if a hurricane's eye is located at 30.5°N on track 11, which is forecast as the most probable track that the hurricane is going to take. The other tracks on each side of track 11 are also possible though their weight is getting smaller away from the center (Figure 14a). If the weight is given to 50% for the track 11 and 10% for the outermost track on both sides, and the hurricane has the same features as in Ex 1, the probability of being inundated in Charleston Harbor and its adjacent coast is shown in Figure 14b. Of course, this is just a simple example of a real case. Fortunately, National Weather Service has already developed a systematic methodology on how to determine 10, 30, and 50 percent strike probability envelope and a cone of uncertainty along the forecast track. This kind of forecast can be made long before the hurricane approaches the coast, when the hurricane's landfall track and location are not quite certain. Whenever they are determined, the forecast hurricane track and other associated information can be input into the model to get the final storm surge and inundation distribution maps as what have been extensively discussed.

[79] **Acknowledgments.** This study is supported by the Carolina Coastal Ocean Observation and Prediction System (Caro-COOPS) project under NOAA grant NA16RP2543 via the National Ocean Service, through Charleston Coastal Services Center. Caro-COOPS is a partnership between the University of South Carolina and North Carolina State University. We thank Madilyn Fletcher and Earle Buckley for constructive comments and project coordination, Shaowu Bao for helpful discussions on the hurricane wind model, and Jeremy Cothran, Braxton Davis, and Charlton Purvis for providing water level and flooding data for Hurricane Hugo, as well as assisting in model verification.

References

- Finley, R. J. (1976), Hydraulics and dynamics of North Inlet, South Carolina 1974–1975, *GITI Rep. 10*, Coastal Eng. Res. Cent., Fort Belvoir, Va.
- Fox, M., and S. J. Maskell (1995), Two-way interactive nesting of primitive equation ocean models with topography, *J. Phys. Oceanogr.*, *25*, 2977–2996.
- Holland, G. J. (1980), An analytic model of the wind and pressure profiles in hurricanes, *Mon. Weather Rev.*, *108*, 1212–1218.
- Houston, S. H., W. A. Shaffer, M. D. Powell, and J. Chen (1999), Comparisons of HRD and SLOSH surface wind fields in hurricanes: Implications for storm surge modeling, *Weather Forecasting*, *14*, 671–686.
- Hsu, S. A., and Z. Yan (1998), A note on the radius of maximum wind for hurricanes, *J. Coastal Res.*, *14*(2), 667–668.
- Hubbert, G. D., and K. L. McInnes (1999), A storm surge model for coastal planning and impact studies, *J. Coastal Res.*, *15*(1), 168–185.
- Jelesnianski, C. P. (1972), SPLASH (Special program to List Amplitudes of Surges From Hurricanes), *NOAA Tech. Memo. NWS TDL-46*, Natl. Oceanic and Atmos. Admin., Silver Spring, Md.
- Jelesnianski, B. R., J. Chen, W. A. Shaffer, and A. J. Gilad (1984), SLOSH: A hurricane storm surge forecast model, paper presented at Oceans 84, Mar. Technol. Soc., Washington, D. C.
- Jelesnianski, C. P., J. Chen, and W. Shaffer (1992), Slosh: Sea, Lake, and Overland Surges from Hurricanes, *NOAA Tech. Rep. NWS 48*, Natl. Oceanic and Atmos. Admin., Silver Spring, Md.
- Kim, S. K., P. L.-F. Liu, and J. A. Liggett (1983), Boundary integral equation solutions for solitary wave generation propagation and runup, *Coastal Eng.*, *7*, 299–317.
- Kjerfve, B., J. E. Greer, and R. L. Crout (1978), Low-frequency response of estuarine sea level to non-local forcing, in *Estuarine Interactions*, edited by M. L. Wiley, pp. 497–513, Elsevier, New York.
- Large, W. G., and S. Pond (1981), Open ocean momentum fluxes in moderate to strong winds, *J. Phys. Oceanogr.*, *11*, 324–336.
- Mellor, G. L. (1996), *User's Guide for a Three-Dimensional, Primitive Equation, Numerical Ocean Model*, Princeton Univ. Press, Princeton, N. J.
- National Oceanic and Atmospheric Administration (NOAA) (1989), Hurricane Hugo: Effects on water levels and storm surge recorded at NOAA/National Ocean Service water level stations, *NOAA Tech. Memo. NOS OMA Data Rep. 1989*, Natl. Ocean Serv., Rockville, Md.
- Oey, L.-Y. (2005), A wetting and drying scheme for POM, *Ocean Modell.*, *9*, 133–150.
- Pedersen, G., and B. Gjevik (1983), Runup of solitary waves, *J. Fluid Mech.*, *135*, 283–290.
- Peng, M., L. Xie, and L. Pietrafesa (2004), A numerical study of storm surge and inundation in the Croatan-Albemarle-Pamlico estuary system, *Estuarine Coastal Shelf Sci.*, *59*, 121–137.
- Phadke, A., C. Martino, K. F. Cheung, and S. H. Houston (2003), Modeling of tropical cyclone winds and waves for emergency management, *Ocean Eng.*, *30*, 553–578.
- Pietrafesa, L. J., G. S. Janowitz, T.-Y. Chao, R. H. Weisberg, F. Askari, and E. Noble (1986), The physical oceanography of the Pamlico Sound, *Sea Grant Publ. UNC-WP-86-5*, Univ. of N. C., Raleigh, N. C.
- Spall, M. A., and W. R. Holland (1991), A nested primitive equation model for oceanic applications, *J. Phys. Oceanogr.*, *21*, 205–220.
- Synolakis, C. E. (1987), The runup of solitary waves, *J. Fluid Mech.*, *185*, 523–545.
- Xie, L., L. Pietrafesa, and M. Peng (2004), Incorporation of a mass-conserving inundation scheme into a three-dimensional storm surge model, *J. Coastal Res.*, *20*, 1209–1223.

M. Peng and L. Xie, Department of Marine, Earth, and Atmospheric Sciences, North Carolina State University, Box 8208, Raleigh, NC 27695–8208, USA. (mpeng@ncsu.edu)

L. J. Pietrafesa, College of Physical and Mathematical Sciences, North Carolina State University, Box 8201, Raleigh, NC 27695–8208, USA.